

Gelation Kinetics and Mechanism of PBLG/Toluene Organogels

by

Merve KOCAKUŞAKOĞULLARI

**A Thesis Submitted to the
Graduate School of Engineering
in Partial Fulfillment of the Requirements for
the Degree of**

Master of Science

in

Material Science and Engineering

Koç University

May 2011

Koc University
Graduate School of Sciences and Engineering

This is to certify that I have examined this copy of a master's thesis by

Merve KOCAKUŞAKOĞULLARI

and have found that it is complete and satisfactory in all respects,
and that any and all revisions required by the final
examining committee have been made.

Committee Members:

Prof. Dr. Adem Levent Demirel (Advisor)

Prof. Dr. Oğuz Okay

Asst. Prof. Dr. Uğur Ünal

Date:

Abstract

Poly (γ -benzyl-L-glutamate) (PBLG) is a synthetic polypeptide which can form thermoreversible organogels with common organic solvents such as toluene. In this thesis, thermoreversible gelation of PBLG has been studied by dynamic light scattering (DLS), micro-viscometer, differential scanning calorimetry (DSC), and ultraviolet-visible spectrometer. In this model system, to understand how rodlike polypeptides form a gel, we have investigated the effect of time, temperature, concentration and addition of other competing molecules. PBLG can form thermoreversible gels in toluene above the critical concentration which was determined to be 4-5 mg/ml close to critical gelation temperature which was found to be between 23°-26°C. The transition temperatures for PBLG/toluene solutions were determined as 51.04°C and 19.65°C by DSC. The time required for gelation of PBLG at different temperatures, decreased with concentration. With increasing PBLG concentration, aggregate size, viscosity and scattered light intensity increased due to growth of aggregates. Turbidity measurements by means of UV-visible spectrometer showed that macroscopic gel was formed only when aggregates fused to each other. From the comparison of the data obtained by different techniques, it was found that each technique was sensitive to different stages of gelation in time. Though onset of PBLG gelation could be detected via DLS, growth of aggregates could be followed by viscometer. Last stage in which the system formed a macroscopic gel could only be observed by turbidity measurements using UV-visible Spectrometer. We propose a model for the gelation of PBLG molecules in toluene in time. Turbidity measurements as a function of time for different concentrations of PBLG/toluene solutions were analyzed on the basis of Avrami equation. The Avrami exponent n was found to be between 2-5 depending on PBLG/toluene concentration indicating different growth mechanisms.

It has been achieved to incorporate polystyrene (PS) into PBLG/toluene solutions with high loading percentages. The critical concentration above which PBLG does not form

macroscopic gel was determined as 82% by weight. Incorporation of PS did not affect the thermoreversibility of PBLG/toluene solutions. DLS results of PS-PBLG/toluene solutions were similar with PBLG/toluene solutions. This indicates that PS has no significant effect on the onset of structure formation which is the first stage of gelation. On the other hand, PS plays a key role in growth of aggregates and their fusion to each other at the later stages of gelation. Network formation of PBLG in PS matrix was confirmed by microscopic measurements.

ÖZET

Poli(γ -benzil-L-glutamat) (PBLG) tolüen gibi organik çözücülerde sıcaklıkla tersinir organojel oluşturan sentetik bir polipeptittir. Bu tezde, PBLG'nin sıcaklıkla kontrol edilebilen tersinir jel oluşturması dinamik ışık saçılımı (DLS), micro-viskozimetre, diferansiyel taramalı kalorimetre (DSC) ve ultraviyole ve görünür ışık (UV-Vis) spektrometresi ile incelenmiştir. Bu model sistemde, zaman, sıcaklık, konsantrasyon ve farklı molekül ilavesinin çubuk şeklindeki polipeptitlerin jel oluşturmaya etkisi incelenmiştir. PBLG, 4-5 mg/ml olarak belirlenen kritik konsantrasyon üzerinde ve 23-26°C olarak belirlenen kritik jelleşme sıcaklığında tersinir organojel oluşturur. PBLG-tolüen sisteminin faz geçiş sıcaklıkları DSC ile 51.04°C ve 19.65°C olarak belirlenmiştir. PBLG'nin farklı sıcaklıklarda jel oluşturması için gereken zamanın konsantrasyonla azaldığı bulunmuştur. Artan PBLG konsantrasyonu ile birlikte, topak boyutu, viskozite ve saçılan ışığın şiddeti artmaktadır. Ultraviyole ve görünür ışık (UV-Vis) absorpsiyon spektrometresi ile yapılan bulanıklık ölçümü, makroskopik jelin topakların birleşmesiyle oluştuğunu göstermektedir. Kullanılan farklı ölçüm tekniklerinin karşılaştırılması sonucunda, her bir tekniğin jelleşmenin farklı bir evresine duyarlı olduğu belirlenmiştir. Jelleşmenin başlangıcı DLS ile belirlenebildiği halde, topakların büyümesi viskozimetri ile takip edilebilmiştir. Makroskopik jelleşmenin son evresi sadece ultraviyole ve görünür ışık (UV-Vis) absorpsiyon spektrometresi kullanılarak yapılan bulanıklık ölçümüyle gözlenmiştir. Bu ölçümlere dayanarak, PBLG moleküllerinin tolüen içinde zamanla jel oluşturmaya açıklayan bir model önerdik. Farklı konsantrasyonlardaki PBLG tolüen çözeltilerinin zamanla değişen bulanıklık ölçümleri Avrami denklemiyle analiz edilmiştir. PBLG/tolüen konsantrasyonuna bağlı olarak Avrami üstelinin, n , 2-5 arasında değişmesi farklı büyüme mekanizmalarına işaret etmektedir.

Polistiren (PS)'in PBLG/tolüen çözeltilerine yüksek oranda ilave edilebilmesi başarılmıştır. PBLG'nin makroskopik jel oluşturmadığı kritik PS konsantrasyonu

ağırlıkça %82 olarak belirlenmiştir. PS'in PBLG/tolüen çözeltilerine katılması sıcaklıkla tersinir jel oluşmasını etkilememiştir. PS-PBLG/tolüen ve PBLG/tolüen çözeltilerinin DLS sonuçları benzerdir. Bu sonuç, PS'in yapı oluşumunun ilk evresine kaydadeğer bir etkisinin olmadığını göstermektedir. Buna karşılık, toprakların büyümesi ve birleşmesi evrelerinde PS'in büyük bir rolü vardır. Yüksek miktarda PS içeren çözeltide PBLG'nin PS matrisi içinde 3 boyutlu ağ yapı oluşturduğu mikroskopik ölçümlerle doğrulanmıştır.

Table of Contents

ABSTRACT	iii
FIGURES	ix
SCHEMES	xii
TABLES	xiii
CHAPTER 1 INTRODUCTION & LITERATURE REVIEW	1
1.1 OVERVIEW OF GELS	1
1.2 HYDROGELS.....	6
1.3 ORGANOGELS	8
1.4 THERMOREVERSIBLE GELATION OF PBLG IN ORGANIC SOLVENTS.....	12
CHAPTER 2 EXPERIMENTAL DETAILS	17
2.1 PBLG ORGANOGELS	17
2.1.1 <i>Materials</i>	17
2.1.2 <i>Preparation of PBLG organogels</i>	17
2.1.3 <i>Preparation of PBLG/PS composite organogels</i>	17
2.1.4 <i>Determination of Critical Gelation Temperature & Concentration of PBLG gels</i>	17
2.2 DYNAMIC LIGHT SCATTERING (DLS).....	18
2.3 ULTRAVIOLET-VISIBLE ABSORPTION SPECTROSCOPY	21
2.4 VISCOSITY MEASUREMENTS.....	23
2.5 INFRARED SPECTROSCOPY	24
2.6 OPTICAL MICROSCOPE.....	25
2.7 DIFFERENTIAL SCANNING CALORIMETRY (DSC)	25
2.8 ATOMIC FORCE MICROSCOPY (AFM).....	26
CHAPTER 3 PBLG/TOLUENE GELS	27
3.1 MOTIVATION	27
3.2 RESULTS&DISCUSSION	28
3.2.1 <i>Determination of Critical Concentration and Temperature for Gelation</i>	28
3.2.2 <i>Determination of critical temperatures by DSC</i>	31
3.2.3 <i>Gelation Kinetics as Observed by DLS Measurements</i>	33

3.2.4	<i>Viscosity Measurements</i>	40
3.2.5	<i>Turbidity Measurements by UV-Visible Spectrometer</i>	42
3.2.6	<i>FT-IR measurements</i>	51
3.2.7	<i>Optical Microscopy Investigations</i>	53
3.2.8	<i>Morphological Investigations of PBLG Gels by AFM</i>	55
CHAPTER 4	PBLG-PS /TOLUENE GELS	57
4.1	MOTIVATION	57
4.2	RESULTS & DISCUSSION	58
4.2.1	<i>Effect of PS concentration on Gelation</i>	58
4.2.2	<i>Determination of PS effect on gelation by DSC Measurement</i>	59
4.2.3	<i>Investigation of PS effect on gelation kinetics by DLS</i>	61
4.2.4	<i>Viscosity Measurements of PS/PBLG organogels</i>	66
4.2.5	<i>Turbidity Measurements of PS-PBLG gels by UV-Visible Spectrometer</i>	68
4.2.6	<i>Optical Microscopy Investigations for PS-PBLG organogels</i>	71
4.2.7	<i>Morphological Investigations of PS-PBLG Gels by AFM</i>	72
CHAPTER 5	CONCLUSIONS	74
	BIBLIOGRAPHY	79
	VITA	85




FIGURES

Figure 1.1 Photograph of a gel (a) and a solution (b)	5
Figure 1.2 Low Molecular Weight Organogels classified due to their nature of networks; (A) Solid-matrix having pseudocrystalline junctions (B) Fluid Matrix having a transient network done by physical entanglements [3].....	10
Figure 1.3 Typical phase diagram for rod-like polymer solution indicating all the three phases : isotropic (I), liquid crystalline (LC) and biphasic (I+LC).....	13
Figure 2.1 UV-Visible Spectrum of PBLG/toluene solution.....	22
Figure 3.1 5.0 mg/ml PBLG in toluene was cooled down from 70 °C to (a) 30 °C, (b) 28,5 °C, (c) 26 °C and (d) 23 °C. The solutions were kept at specified temperatures for 2 h and then the vials were turned upside down. Only in (d) a macroscopic gel was formed which did not flow down against gravity.	29
Figure 3.2 Homogeneous PBLG-toluene solutions having concentrations of 1.0 mg/ml (a), 2.0 mg/ml (b), 3.0 mg/ml (c), 4.0 mg/ml (d) and 5.0 mg/ml (e) respectively. The solutions were kept at 23°C for 2 h and then the samples were subjected to gravity. Only in (d) macroscopic gel was formed which did not flow down against gravity.	30
Figure 3.3 Heating and cooling DSC cycles of 10 mg/ml PBLG-toluene solution. Exothermic peak at 19.65°C corresponds to gelation of PBLG-toluene solution and endothermic peak at 51.04°C corresponds to melting of PBLG gel. Scan rate was 5°C/min.	32
Figure 3.4 Optical photos of 5 mg/ml PBLG-toluene gels which were kept at (a) 23°C, (b) 30 , (c) 50°C and (d) 70°C for 2 h. In (a) and (b) macroscopic gels did not move down against gravity. (c) corresponds to viscous fluid which lost its stability and (d) corresponds to homogenous PBLG solution.	33
Figure 3.5 Aggregate size growth as a function of time measured for homogeneous PBLG- toluene solutions having concentrations of (a) 0.4 mg/ml, (b) 1.0 mg/ml, (c) 3.0 mg/ml and (d) 5.0 mg/ml recorded at 26°C. The size of first peak is represented by (■) and second peak is represented by (●)	35
Figure 3.6 Aggregate size growth as a function of time measured for homogeneous PBLG- toluene solutions having concentration of 5.0 mg/ml recorded at (a) 30°C, (b) 28.5°C, (c) 27°C and (d) 26°C. The size of first peak is represented by (■) and second peak is represented by (●).....	38
Figure 3.7 Time dependency of viscosities of 0.4 mg/ml (▲), 1.0 mg/ml (▲), 3 mg/ml (■) and 5 mg/ml (●) PBLG/toluene solutions at 26°C.....	41
Figure 3.8 Time dependent evolution of the UV-Visible Spectra of 5.0 mg/ml PBLG/toluene solution recorded at 23°C over a 2 hour period.	43

Figure 3.9 Turbidity curves showing aggregate formation of PBLG/toluene solutions having concentrations of 0.4 mg/ml (■), 1.0 mg/ml (●), 3.0 mg/ml (▲) and 5.0 mg/ml (▲) over time. Data were collected at 600 nm since cooling from 70°C to 23°C.....	44
Figure 3.10 Determination of gelation time (t_g) and change in absorbance (ΔA) from sigmoidal fit to the UV-Vis data of Fig. 3.9.	45
Figure 3.11 Critical time for gelation (■) and change in absorbance (■) as a function of PBLG/toluene concentration. Determination was done by applying sigmoid fit to specified concentrations as shown in Fig. 3.10.....	46
Figure 3.12 Turbidity curves showing aggregate formation of 5 mg/ml PBLG/toluene solutions which were cooled down from 70°C to 23°C (●) and 26°C (■). Data were collected at 600 nm.	48
Figure 3.13 Gelation kinetics of 5 mg/ml PBLG/toluene solutions at 23°C (■), 24°C (●), 25°C (▲) (a) and fit of Avrami equation (b), Gelation kinetics of PBLG/toluene solutions with concentration of 0.4 mg/ml (■), 1.0 mg/ml (●), 3.0 mg/ml (▲) at 23°C (c) and fit of Avrami equation (d).	49
Figure 3.14 FTIR spectrum of dried PBLG/toluene gel prepared from 5 mg/ml solution by solvent casting. Measurement was taken at room temperature.	52
Figure 3.15 Optical microscopy images of PBLG toluene solutions; aggregated PBLG formed by spin coating at room temperature (a), 30 mg/ml PBLG-toluene gel obtained by drop casting on a glass slide at room temperature (b) and its crystalline structure under polarized light (c).	54
Figure 3.16 AFM micrographs of spin coated PBLG/toluene gel with concentration of 0.4 mg/ml shown as 20 μm scan (height) (a), 5 μm scan (height) (b) and 5 μm scan (phase) (c), respectively.	55
Figure 4.1 Heating and cooling DSC cycles of 10 mg/ml PBLG-toluene composite gel including 60% PS. Exothermic peak at 21.38°C corresponds to gelation and endothermic peak at 53.11°C corresponds to melting transition. Scan rate was 5°C/min.	60
Figure 4.2 Aggregate size growth as a function of time measured for homogeneous 5 mg/ml PBLG-toluene solutions containing (a) 0.4%, (b) 0.6%, (c) 0.8% and (d) 1.0% PS recorded at 26°C. The size of first peak is represented by (■) and second peak is represented by (●).....	62
Figure 4.3 Aggregate size growth as a function of time measured for homogeneous 5 mg/ml PBLG-toluene solutions containing (a) 0.4%, (b) 0.6%, (c) 0.8% and (d) 1.0% PS recorded at 30°C. The size of first peak is represented by (■) and second peak is represented by (●).....	64
Figure 4.4 Aggregate size growth as a function of time measured for homogeneous 3 mg/ml PBLG-toluene solutions containing (a) 60% PS and (b) 0% recorded at 26°C. The size of first peak is represented by (■) and second peak is represented by (●).....	65

<i>Figure 4.5 Time dependency of viscosities of 5.0 mg/ml PBLG/toluene solution (■) and 5.0 mg/ml PS-PBLG/toluene solution containing 60% PS by weight (●) at 26°C.</i>	<i>67</i>
<i>Figure 4.6 Turbidity curves showing aggregate formation of 5 mg/ml PBLG/toluene solutions containing %1 (■), 2% (●), 0%(▲)and 60% (▲) PS as a function of time. Data were collected at 600 nm since cooling from 70°C to 23°C.</i>	<i>68</i>
<i>Figure 4.7 Critical time for gelation (■) and change in absorbance (●) as a function of loading percentage of PS. Determination was done by applying sigmoid fit to 5 mg/ml PBLG/toluene solutions containing 0%, 1%, 2% and 60% PS as shown Error! Reference source not found..</i>	<i>70</i>
<i>Figure 4.8 Optical micrograph of dried PS-PBLG organogel under crossed polarized light. Arrows indicated the fibrillar network of the residue.....</i>	<i>71</i>
<i>Figure 4.9 AFM height (a) and phase (b) images of spin coated PBLG gel from 0.4 mg/ml PBLG/toluene solution including 60%PS.</i>	<i>72</i>
<i>Figure 5.1 Model proposed for gelation of PBLG in toluene</i>	<i>76</i>

Schemes

<i>Scheme 1.1 Representation of a) Chemically bonded gels b) Physically bonded gels</i>	<i>polymer,</i>	
<i>liquid</i>	 <i>molecule,</i>	 <i>covalent bond,</i>
		 <i>non-covalent bond..... 2</i>
<i>Scheme 1.2 Classification of Gels</i>		<i>..... 4</i>
<i>Scheme 1.3 Examples of polymers which have LCST near body temperature [15]</i>		<i>..... 6</i>
<i>Scheme 1.4 Molecular structure of PBLG (a), Computer generated 3D structure for PBLG [33] (b) and representation of intramolecular hydrogen bonding [34] (c).</i>		<i>..... 12</i>
<i>Scheme 2.1 Representation of propagated waves when the light interacts with the particles [50].</i>		<i>..... 19</i>
<i>Scheme 2.2 A typical correlation function against time [50].</i>		<i>..... 20</i>
<i>Scheme 4.1 Diagram showing the state of PBLG-PS/toluene solution depending on loading percentage of PS. The homogenized solutions were kept at 23°C for 2 h and then subjected to gravity. The experimental data shown as</i>		<i>..... 58</i>

Tables

<i>Table 3-1 The avrami exponents (n) as function of temperature (T) for 5 mg/ml PBLG/toluene solutions.</i>	50
<i>Table 3-2 The avrami exponents (n) as function of concentration (C) at 23°C.</i>	50
<i>Table 3-3 Comparison of Vibrational Frequencies for Structured PBLG and Bulk PBLG (Literature).</i>	53

Chapter 1 Introduction & Literature Review

1.1 Overview of Gels

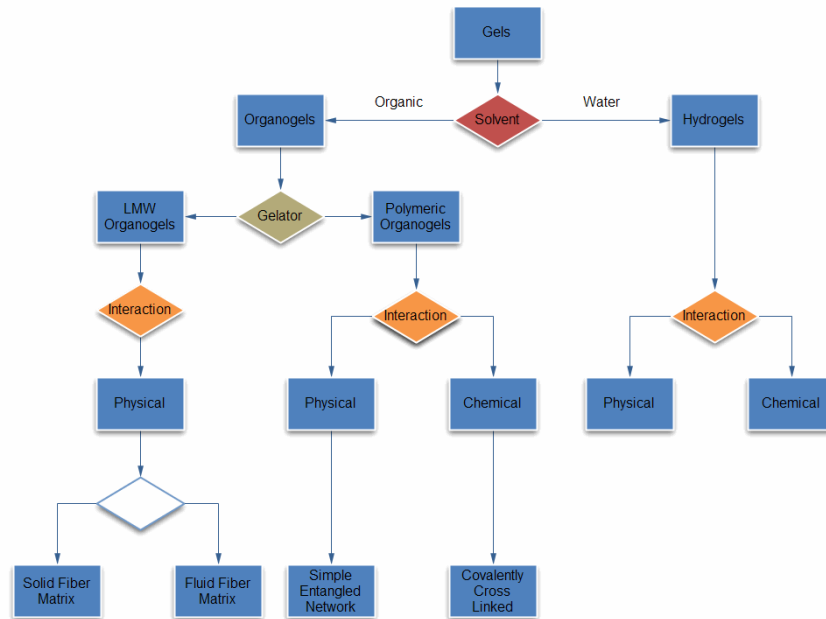
In recent years soft matter research has gained much attention due to their various application areas in pharmaceutical, cosmetic, chemical and food industry [1]. Soft matter systems consist of liquid crystals, micelles, polymers, gels, foams and biomolecules. Among these, gels are unique in that they hold a huge amount of liquid within a 3-dimensional (3D) network structure formed by only a small amount of gel forming substances called gelators [2]. The required amount of gelator to immobilize the liquid medium is quite low, typically less than 15 % by weight [3]. Although these systems contain predominantly liquid, the surface of the network structure provides strong interactions to capture the liquid molecules. Immobilization of liquid molecules by the gelator network causes an increase in viscosity and a yield stress. Such systems are referred as viscoelastic materials due to having both viscous and elastic characteristics. Gel systems show solid-like properties at small deformations in their mechanical response.

In a gel, depending on the gelator molecules, the gelling matrix may contain water or an organic liquid. Accordingly, the priori classification of gels is done concerning the solvent nature which disperses in the gel network. If gelation occurs in the presence of water, system is named as “hydrogel”. Otherwise, gel is referred as “organogel” which differs from hydrogels by their predominantly organic medium. Further subclassification of gels can be done based on the nature of the gelling agent. The common gel forming substances include polymers and low molecular mass molecules. These gelators can construct mesh-like network through chemical cross-links [4] or physical interactions [5]. The intermolecular interactions of gelator molecules in the medium of the liquid trigger 3D network formation and then the interactions between the surface of the network structure and the liquid molecules cause the trapping of the

external stimuli and show reversible sol-gel transitions due to weaker interactions that hold the 3D network together. Nature of the interactions in between gelator molecules allows the system to undergo phase transition in the presence of external stimuli. Their physical connection points may respond to pH, electric field, temperature, light or other external stimuli [7]. Due to sensitivity to external stimuli, physical gels can change their shape in 2D or 3D [7]. This phenomenon provides many application areas to stimuli-responsive physical gels such as drug delivery, pharmacy and tissue engineering.

In the case of gel formation through physical interactions, gelation process begins with self-assembly of molecules forming mesh-like network and then continues by entrapping liquid molecules in micro- or nano-spaces of this structure. The interactions governing self-assembly of gelator molecules in solvent can be hydrogen bonding, π - π stacking, electrostatic or van der Waals interactions [8].

Polymers are good candidates for gelling agent to obtain either hydrogels or organogels. In addition to polymers, organogels can be also formed by Low Molecular Weight Organogelator molecules (LMOG)s. A flow chart given below summarizes the classes of gels due to nature of solvent, interactions and gelators.



Scheme 1.2 Classification of Gels

As mentioned before, gels are viscoelastic materials, sometimes called as soft-solid materials. They display solid like properties at low deformations such as elastic response and yield stress. They do not show steady state flow and have well-defined shapes [9]. Many attempts have been made to design gels having high mechanical strength [6, 10, 11]. Rheological investigation of gels in terms of storage modulus, $G'(\omega)$ and loss modulus, $G''(\omega)$ is common to understand their viscoelastic properties[7].

When stress is applied to gels, they store some of the energy and the rest is dissipated [9]. The stored energy in the 3D network of the system is utilized for recovering part of its deformation when stress is taken away. The elastic behavior of gels originates from the network structure. The applied stress stretches the physically or chemically cross-linked network. If the network structure is not disrupted, gels can recover their shape when the applied stress is removed. Gels undergo plastic deformation if and only if the

physical or chemical bonds holding the network structure together is disrupted. Therefore, the mechanical strength of gel systems depends significantly on the strength of the bonds between the gelator molecules in the network.

Besides their mechanical properties, puzzling formation mechanism of supramolecular gels also intrigues scientists. Gelation begins with structure formation of gelators by self-assembly in the medium of the liquid. The growing structures branch out or entangle to form 3D network.

Gelation mechanism is considered as the most challenging question about physical gels to be answered [12]. The cliché definition “easier to recognize than define” may emphasize the complexity of understanding gel formation mechanism [13]. Indeed, recognizing a gel is easy by inverting the container and observing whether the sample flows or not.

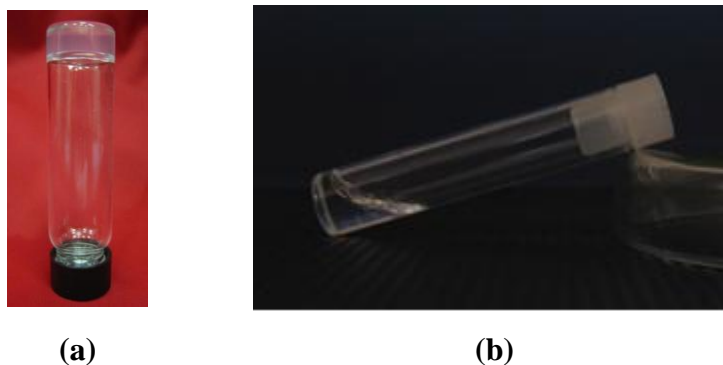
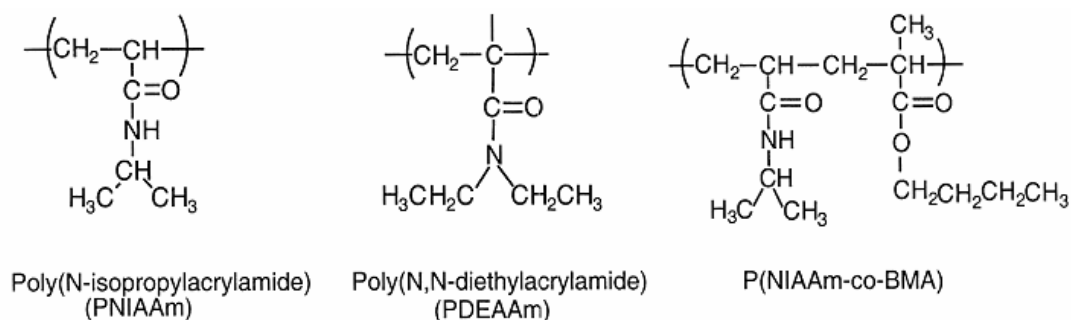


Figure 1.1 Photograph of a gel (a) and a solution (b)

However, understanding the organization stages of supramolecular gelation is quite challenging. Non-covalent interactions, entanglement and the growth of structure in time still await definite answers. The understanding of gelation mechanism and kinetics is important to be able to tune gel properties such as critical gelation temperature, sizes of structures etc. according to the application requirements.

1.2 Hydrogels

Hydrogels are one group of the soft materials formed by the combination of hydrophilic polymers and water which is the dispersant medium. The physical properties of hydrogels such as stimuli-sensitivity, degradability, porosity make them intriguing for the design of smart systems. For instance, a temperature sensitive hydrogel can be designed for *in vivo* drug delivery purposes using a polymer having a critical transition temperature that is close to the body temperature. For such applications, poly(N-isopropylacrylamide) which has lower critical solution temperature (LCST) of 33°C has long been used [14]. The polymers having LCST in the range of 30-40°C are good candidates for controlled-release drug delivery systems thereby their sol-gel transition can take place at the human body [14].



Scheme 1.3 Examples of polymers which have LCST near body temperature [15]

Besides temperature responsiveness, it is possible to design hydrogels with different physical properties and different applications such as [16].

- Solid-like forms (e.g., soft contact lenses),
- Powdered appearance (e.g., pills or capsules for oral ingestion),
- Microparticles (e.g., as bioadhesive carriers or wound treatments)
- Coatings (e.g. implants)
- Membranes or sheets

In contrast to wide application areas, there have been some problematic issues related to the practical utilization of hydrogels. Major problems include fragility, biocompatibility and biodegradability, limited swelling ratio and sterilization issues. All these decrease the feasibility of the gel systems during applications. The recent studies on hydrogels proposed that they significantly suffer from low mechanical strength [16]. There are ongoing studies which try to enhance the strength of hydrogels. Gong et al. [11] reported a very tough hydrogel containing Poly-2 acrylamido-2 methylpropane sulfonic acid (PAMPS) /Poly-acrylamide (PAAM) which is resistant to damage. The gel is obtained by the incorporation of second polymer (PAAM) to the system (PAMPS-water) via crosslinking. The authors proposed that inducing second polymer to hydrogel system increases the material's mechanical strength dramatically.

Last but not least, improving the rheological properties of hydrogels is also possible with the incorporation of additives and additional physical interactions. These kinds of interactions are mainly based on the dispersion of additives in the solvent rich phase. The physical interactions between additional particles and gel system can bring unique properties to hydrogel such as sensitivity to pH, temperature, light etc. In 2007, the incorporation of Single Walled Carbon Nanotubes (SWCNT)s to a supramolecular gel was reported [17]. It is noteworthy that this research was the first article in the literature that demonstrates the attachment of SWCNTs to a hydrogel system physically. The authors managed to form a hybrid supramolecular gel which needed shorter gelation time with respect to the native one. However, latter work has shown a significant disadvantage; a decrease in mechanical strength was observed with addition of SWCNTs. The strengthening of hydrogels and tuning their physical properties via incorporation of additional materials are quite common in this exciting field.

Research on gels has been mainly dominated by the hydrogels due to their biological and medical applications. By designing hydrogels, various smart materials can be fabricated in order to utilize in diverse application areas such as tissue engineering,

microfluidic systems, drug delivery and so on. One promising polymer exhibiting thermoreversible behavior, poly (N-isopropyl acrylamide) PNIPAAm is utilized as actuating devices in order to induce shape deformations of cells. In this work, Pelah et al. loaded highly deformable blood cells in between PNIPAAm hydrogel and glass [18]. In the case of temperature increase above LCST, polymer shrinks and forms a gel network which causes deformation of blood cells. Such systems have an advantage that provides an opportunity to manipulate structure and function of biomolecules and cells.

1.3 Organogels

Organogels, the main focus of this thesis, are comprised of gelling agent and an entrapped organic liquid phase. In organogels, gelator molecules can be either polymers or Low Molecular Weight Organogelators (LMWOG)s. Like hydrogels, organogels contain mesh-like network formed by restructured gelator molecules. The organization of these structures is triggered by covalent or non-covalent interactions between the molecules. Research on organogels have been largely dominated by LMW organogels because of their thermal reversibility and self-assembling ability [19].

Various questions about stimuli-responsive organogels are still to be answered, such as tuning physical properties e.g. gelation temperature, explaining thermodynamics of organogels, additive effect on physical properties, controlling organization stages and enhancing rheological properties of organogels. In the literature, there have been diverse studies associated with these subjects. Moniruzzaman et al. have produced an organogel/carbon nanotubes (CNT)s composite system that displayed higher mechanical strength compared to the native one. The system was composed of multi walled carboxylated CNTs as additive, 12-hydroxystearic acid (HSA) as the gelator molecules and 1,2-dichlorobenzene as the liquid phase. They found that the existence of CNTs increases the organogel's mechanical strength. The authors explained the improvement in mechanical strength in terms of the hydrogen bonding interactions which take place between carboxylated CNTs and gelator molecules. Another work

highlights a kinetic study on the self-assembly gelation mechanism. In this work Liu et al. have examined the formation kinetics of supramolecular organogel “SMGA N-lauroyl-L-glutamic acid di-*n*-butylamide (GP-1)/iso-stearyl alcohol (ISA) via SEM, rheometry and DLS [20]. They proposed a formation process for fractal structure of an organogel network. The mechanism can be described as follows: first the nucleation occurs, and then crystal domains begin to grow. The growing crystalline structure branch out. Finally, the structure extends into 3D mesh-like network. The authors have expressed the self-assembly of the system via Cayley branching tree [21].

LMW organogels are interesting soft materials not only because of their potential applications but also their puzzling gelation mechanism. Self-assembly of organogel structures has been widely studied in recent years [22]. Aggregation of LMW organogels is driven by molecular interactions such as hydrogen bonding, solvophobic effects, van der Waals, electrostatic or π - π stacking interactions. It is difficult to come up with a general interpretation of the gelation mechanism [12] and its reversibility. In case of thermally reversible behavior, temperature affects the interactions between solvent molecules and (LMWOG)s and causes the system to disrupt and form the weak physical interactions [23]. It is possible to determine the phase transition temperature of LMW organogels via Differential Scanning Calorimetry (DSC) or other spectroscopic methods [24]. Various mechanisms were proposed to explain physical transitions of LMW organogels [25]. The morphology of gels can also be discovered by using AFM, STM or SEM.

There are few known facts about gelation mechanism. Firstly, mesh-like network is ordered and can be crystal-like. Depending on the crystalline domains of the network especially at the junction points, LMW organogels are divided into two major groups; *i*) Solid-matrix gels *ii*) Fluid-matrix gels [3]. The network contains junction points typically due to physical entanglements. These junctions can have either large crystal domains or simple entanglements. If crystalline structure is dominant at the junctions,

network becomes more robust. In addition, the matrix behaves more stable like solids and referred as “Solid Matrix”. Fluid-matrix gel originates from intermingled chains. The chain network may disrupt even under very small applied stress. In other words, they are relatively weak compared to solid matrix organogels.

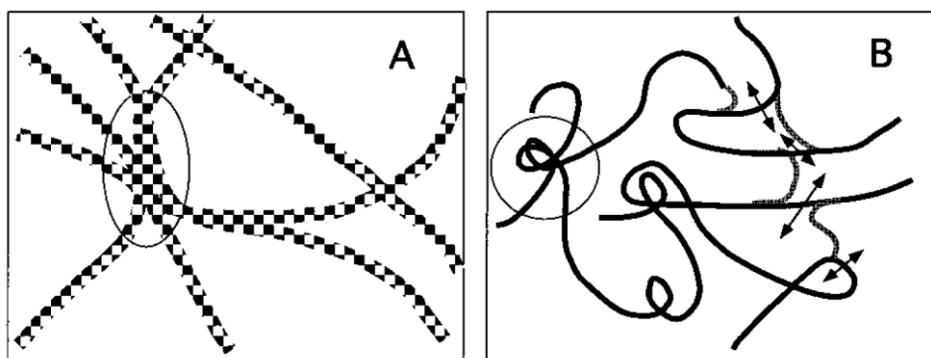


Figure 1.2 Low Molecular Weight Organogels classified due to their nature of networks; (A) Solid-matrix having pseudocrystalline junctions (B) Fluid Matrix having a transient network done by physical entanglements [3].

Gelation of LMW organogels strongly depends on temperature and concentration. Below a critical gelator concentration, system exists as a viscous fluid. Sol-gel transition occurs only at specific temperatures which is important to understand phase diagrams of LMW organogels. Another fact which affects gelation of LMW systems is the chain length of the gelator [19].

LMW organogels can be considered for some applications in industry such as food, medicine, materials science, cosmetic etc. [23]. In particular, thermoreversible character may make LMW organogels good candidate for thermosensors. In contrast to other applications, the toxicology of many organic liquids should be taken into account for pharmaceutical applications. Designing a smart system from LMW organogels for drug delivery is quite difficult with respect to hydrogels. In this case, there are more things that need to be considered;

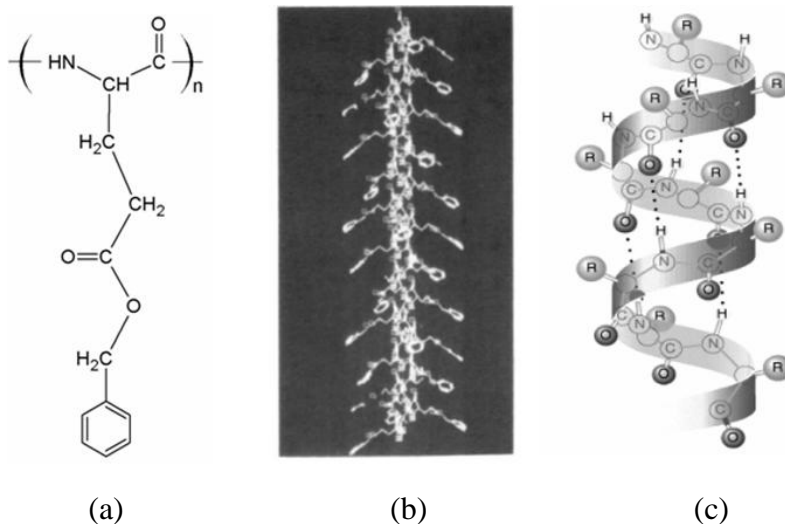
- The possibility of using selected organic solvent in *vivo*
- Predicting suitable gelling agent which may trap the solvent and form gel
- The biocompatibility of gelator.

There are some reported works on organogels for drug delivery applications. Grace et al. investigated formulation of diclofenac in Lecithin organogel which satisfies all the requirements for using in vivo. Due to its amphiphilic character, lecithin forms reverse micelles in oils (isopropyl palmitate, ethyl oleate etc) upon the addition of small amounts of water and when they reach a critical size, they begin to intermingle to each other to form gel network [3]. This has also been commercially available [26]. Another example regarding the potential use of functional organogels has been reported by Karakutuk et al.[4]. They formed a cross-linked macroporous rubber gel in order to remove oil from water surface.

To understand the thermoreversible nature of organogels, liquid crystalline physical gels are in high demand because they exhibit phase transitions and have rod-like structure [23]. Among liquid crystalline (LC) organogels, rod-like organogels were extensively studied as model systems to understand the nature of gelation phenomenon. Although, rod-like molecules lack internal chain flexibility to form crystallites acting as cross-links of the network, they have a capability of forming gels [27]. In this respect, the gel formation begins with arrangement of rigid molecules in an ordered fashion. Furthermore, the packing form of rod molecules governs fiber formation and consequently gel network is obtained in three dimensions. Due to reduction in inter rod interactions, gel loses its solid-like form and undergoes a phase transition resulting in solution. Although there are many definitions of thermoreversible gelation by means of fiber formation, none seems to elucidate fiber growth or fiber gelation exactly. In attempt to explore the sol-gel transition of rod-like polymers, a well-known model system has been widely used. Since the discovery that Poly (γ -benzyl-L-glutamate) (PBLG) solution can form LC organogels [28], it has been the focus of many systematic studies.

1.4 Thermoreversible Gelation of PBLG in Organic Solvents

Poly (γ -benzyl-L-glutamate) (PBLG), which was firstly synthesized in 1930 [29] by Courtaulds, have been widely used as a model of rod-like molecules due to its rigid α -helix structure and liquid crystalline behavior [24]. The molecular structure of PBLG in solution depends on the nature of the solvent. For instance, α -helix conformation of PBLG only exists in liquids which do not disrupt the intramolecular hydrogen bonding. These solvents are called as “helicogenic solvents” i.e. benzyl alcohol, toluene, benzene etc. On the other hand random coil structure requires organic solvents which have capability of interfering intramolecular hydrogen bonds, trifluoroacetic acid (TFA) is a good example. It should be noted that in the case of perturbation of helical backbone, PBLG presents as coil, thus it cannot form 3D network causing gel formation [30]. This indicates that helix structure of PBLG gives rise to gel formation by means of enhancing rigidity of PBLG molecules. The robustness of PBLG structure gives rise to formation of rod-like fibers and then these fibers organize in order to form a network required for gel formation. The fibers have diameters ranging from 0.1 nm to 1 nm (even more), however the initial aligned rods are 0.02 nm in diameter [31].



Scheme 1.4 Molecular structure of PBLG (a), Computer generated 3D structure for PBLG [33] (b) and representation of intramolecular hydrogen bonding [34] (c).

PBLG can form two secondary structures: α -helix or β sheets which depends on liquid medium. The α -helix structure arises from intramolecular hydrogen bonding in between the n^{th} oxygen atom of a carbonyl group and $(n+4)^{\text{th}}$ hydrogen of the amide group [32]. PBLG has a α -helical conformation which is 18/5 [33]. In details, the α -helix of PBLG requires 3.6 residues for one turn (18 residues per 5 turns). One single residue is approximately 0.54 nm in right handed L- α amino acids [33]. Helical structure induces large dipole moment which is parallel to the helical axis [34]. The literature value of the dipole moment for a peptide residue is ~ 3.4 D [35]. If PBLG exhibited such a dipole moment, it would be too stable to go for a phase transition. However there exist some studies which argue that PBLG is rather flexible in solution due to containing amorphous defects on the polypeptide backbone [35]. In other words, these defects are the reason for the phase transition. Dipole moment brings liquid crystalline behavior in to the system In particular, PBLG molecules can be oriented in an ordered fashion however above a certain temperature they can disperse randomly in the solution. This feature is the key issue for phase transition.

Phase transition has been studied by many researchers; however Flory was the first to propose a phase diagram for rod-like polymers [25].

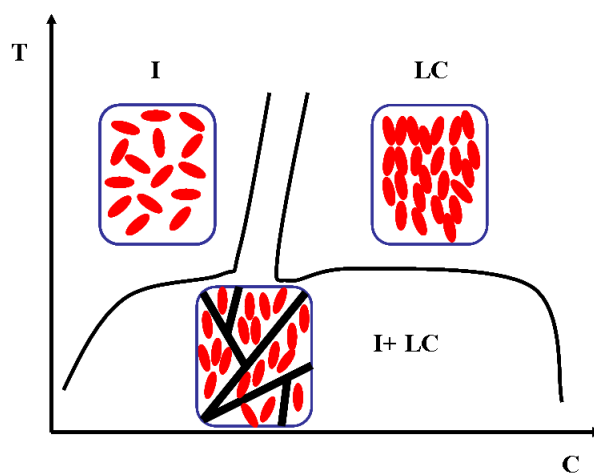


Figure 1.3 Typical phase diagram for rod-like polymer solution indicating all the three phases : isotropic (I), liquid crystalline (LC) and biphasic (I+LC).

Figure 1.3 demonstrates that rod-like polymers such as PBLG can exist in three different phases in a solvent, these are; liquid crystalline (LC) phase for higher concentrations, isotropic phase for lower concentrations and the phase where both LC and isotropic phase can coexist (biphasic region). In addition, biphasic region corresponds to gel formation. In good solvents biphasic region is present for narrower concentration range; however this range increases in the presence of poor solvent [36]. In a sense, poor solvent corresponds to unfavorable solvent in which rod like molecules resist to be dissolved. Gel formation occurs in such solvents through transition from good solvent to poor solvent by means of decreasing temperature. It is remarkable that gel formation is too sensitive to temperature change. Even a small change in temperature (few degrees) can affect the system's behavior in a totally different way.

Thermoreversible gelation of rod-like polymers is a challenging issue which is still needed to be explained. In this regard, the helical polypeptide, poly (γ -benzyl- α -L-glutamate) PBLG, is a good candidate for using as a model system in order to understand this phenomenon. Since PBLG can form gels in many solvents, thermoreversible gelation has been studied in different solvents such as benzene [37], toluene [31], benzyl alcohol [38], DMF [39] and dioxane [30]. Although the literature includes many publications related with nature of PBLG gels, general understanding has still not been achieved. Recent results reveal that mechanism of reversible gels, such as PBLG systems, are remarkably complicated. Yet variety of mechanisms can result in thermoreversible gelation of PBLG in various solvents. In particular two main models regarding phase separation phenomenon of PBLG solutions have been argued by different research groups which are; spinodal decomposition (SD) and nucleation and growth (NG).

Miller et al. explained that gel formed as a result of spinodal decomposition without showing any evidence [31]. In the later work, Miller and co-workers did more quantitative study in order to elucidate gelation of PBLG on the basis of spinodal

decomposition but their measurement technique failed to confirm that [40]. Furthermore Korenaga et al. also suggested that phase separation of PBLG gels were related with spinodal decomposition however they could not find any obvious evidence to support their argument [41]. On the other hand, interestingly, Tipton and Russo did not attribute the gelation model of PBLG solutions to spinodal decomposition in their recent study [36] which is on the contrary of Russo's earlier research [40]. More recently, Tadmor et al. proposed alternative gelation mechanism; nucleation and growth for PBLG aggregates [42]. In addition to these, there have been still other extensive experimental and theoretical studies reported in the literature regarding the phase diagram and the properties of PBLG solutions [43-46]. Mapping out phase diagram of PBLG solutions is quite challenging due to limitations of techniques and the nature of PBLG solutions [31, 40, 45]. Errors in such systems are possible due to extreme sensitivity to the conditions such as, temperature and trace amounts of non-solvent [47]. To achieve a general understanding of thermoreversible gelation of PBLG solutions conditions should be kept definitely constant.

The current study is based on investigating the gelation kinetics rather than phase boundaries of PBLG-toluene solutions by following aggregation stages. The ability of dilute concentration solutions of PBLG to form gels has been known for many years. However concentration, temperature and time effects on aggregation process have not been studied systematically. Although most of the articles published on this subject are based on understanding gelation behavior of PBLG solutions, there is few report in the literature that studies the effect of concentration of PBLG solutions below/around critical gelation concentration. Hereby we focus our study on PBLG-toluene solutions which have concentrations close to critical gelation concentration. In other words kinetics of molecular aggregation is followed by comparing gelling and non-gelling concentrations of PBLG solutions in toluene.

On the other hand, we would like to emphasize that present study is the first report in the literature which aims to investigate molecular aggregation kinetics of PBLG-toluene solutions in the presence of additives. The idea of improving and investigating PBLG gels' physical properties by incorporation of additives is a novel research area which still waits to be explored. Since end to end aggregation of PBLG helices are associated with π - π stacking interactions [46, 48], we use Polystyrene and Single Walled Carbon Nanotubes (SWCNT)s in order to incorporate into PBLG organogel because they possess aromatic moieties.

Since CNTs was discovered by Iijima [49], they have attracted tremendous attention in recent years due to their unique optical, electrical, mechanical and biological properties. In this respect, CNTs become an ideal candidate for gel systems to enhance their mechanical strength and stability. There are recently published articles in the literature concerning fabrication of hydro/organogel nanocomposites containing well-dispersed CNTs [10, 17]. Because CNTs form bundles due to strong intrinsic Van der Waals interactions, dispersion or dissolution can be problematic. To this respect, functionalization of CNTs can be a feasible way to enhance dispersion [10]. However, in our case, PBLG plays an important role in dispersing CNTs and forming organogel without any functionalization. Composite PBLG organogels are achieved by means of physical interactions which takes place in between PBLG and additives. SWCNTs and PS molecules are successfully integrated into PBLG-toluene solutions in order to form composite gels. In this study, aggregation process of hybrid gels and also native gels were monitored by Dynamic Light Scattering, UV-Vis Spectroscopy and Micro-Viscometer. Further investigations were done by Differential Scanning Calorimetry, FT-IR spectroscopy, Optical Microscopy and Atomic Force Microscopy.

Chapter 2 Experimental Details

2.1 PBLG Organogels

2.1.1 Materials

PBLG having molecular weight of 30,000-70,000 g/mol was purchased from Sigma-Aldrich. Atactic Polystyrene (PS) having molecular weight of 2000 g/mol was purchased from Fluka. Toluene with purity 99.9% was obtained from Merck Chemicals and used without further purification.

2.1.2 Preparation of PBLG organogels

PBLG was dissolved in toluene at 70°C and kept at that temperature in an oven for at least 2 hours to ensure a homogeneous solution. The solution was then cooled quickly or quenched below the critical gelation temperature and kept at that temperature for 2 hours for gelation. For visual observations the hot PBLG solution was quenched by putting into a cell kept at 23°C by a Peltier Temperature Controller. Dynamic Light Scattering (DLS), viscosity and UV-Visible absorbance measurements were all carried out at 26 °C.

2.1.3 Preparation of PBLG/PS composite organogels

5 mg PBLG and various amount (0.03 mg to 30 mg) of polystyrene (PS) were dissolved in 1 ml toluene in a closed vial at 70°C for 2 hours. Then, the homogeneous solutions were quenched by putting into a cell kept at 23°C by a Peltier Temperature Controller and kept at that temperature for 2 hours.

2.1.4 Determination of Critical Gelation Temperature & Concentration of PBLG gels

PBLG solutions were prepared in toluene at concentrations of 1.0, 2.0, 3.0, 4.0 and 5.0 mg/ml in closed vials. After keeping the solutions at 70°C, the homogeneous solutions

were kept at different temperatures (30 °C, 27 °C and 23°C) for 2 hours. At the end of 2 hours, the samples were turned upside down and subjected to gravity for 1 hour. The solutions that did not flow down were recorded as gel. Otherwise, they were referred to as viscous solution. The minimum concentration that formed gel at the lowest temperature (23°C) was assigned as the critical concentration. The maximum temperature above which the highest concentration (5 mg/ml) did not form gel was assigned as the critical temperature.

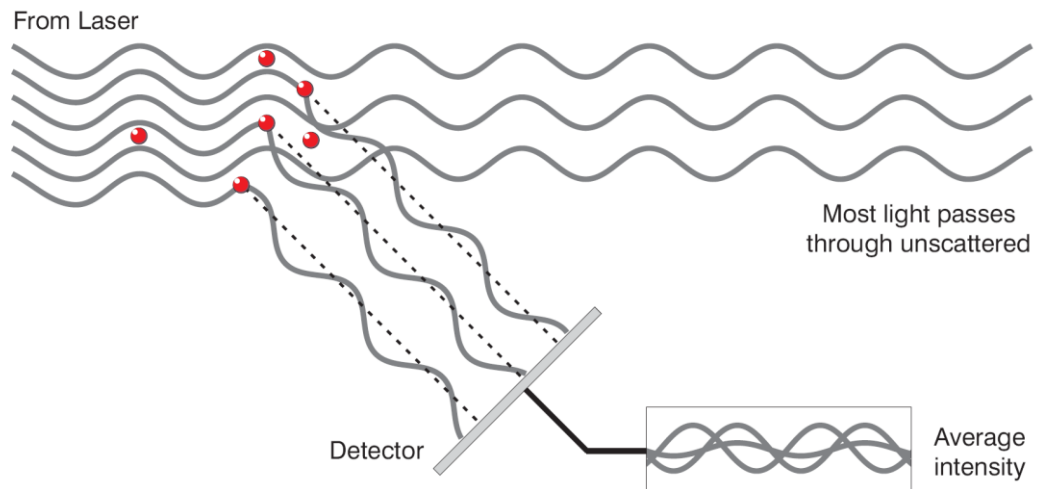
The same procedure that was used for PBLG gels were also used for PBLG/PS gels.

2.2 Dynamic Light Scattering (DLS)

Dynamic Light Scattering is a technique used for determination of particles' diameter. The theory is based on random movement of particles (Brownian motion) dispersed or dissolved in a liquid medium. Brownian motion is the movement of particles due to random collisions with the molecules of liquid which surrounds the particle. According to Brownian motion theory, small particles move more quickly than large particles. In a sense, particle's size is associated with its diffusion rate due to Brownian motion which is an important feature for determining particle's diameter in Dynamic Light Scattering. In DLS, size is calculated by means of Stokes-Einstein theory which gives a relation between diffusion coefficient and the size of a spherical particle undergoing Brownian motion. According to Stokes- Einstein relation, the diameter of the particles (a) is related to the diffusion constant, D, as shown below:

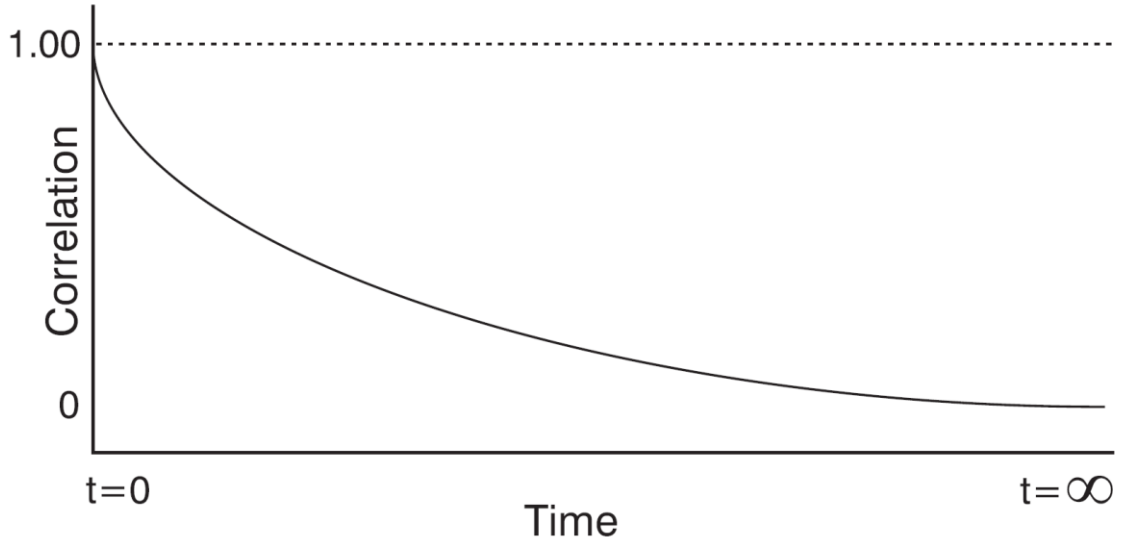
$$D = \frac{k_B T}{6\pi\eta a}$$

where k_B is the Boltzman constant, T is the temperature , η is the viscosity of the medium and a is the diameter of the particles. Using D determined from autocorrelation function (ACF) of scattered intensity, the diameter of particles can be easily calculated if T and η are known.



Scheme 2.1 Representation of propagated waves when the light interacts with the particles [50].

Scheme 2.1 exhibits the propagated waves, when the light beam of the laser interacts with the particles. The intensity of scattered light reaching detector is used in order to analyze average intensity. Scattered light intensity changes with time due to the diffusion of particles in the liquid and therefore the average intensity fluctuates. The fluctuations in scattered intensity are examined through a correlator which basically measures the degree of similarity between scattered light signals over a period of time. At short time intervals the correlation is high since the particles do not have a chance to change their position significantly from the initial state they were in. When the time delays become longer, correlation decays exponentially. The correlation is therefore will eventually reach zero as shown in Scheme 2.2. The smaller particles diffuse faster than the larger particles, so the correlation function decays much faster for smaller particles.



Scheme 2.2 A typical correlation function against time [50].

In order to derive dynamic information about particles movement in a liquid by Brownian motion, autocorrelation function is used. The data is analyzed through autocorrelation function ($g^{(2)}(q,t)$) with the aid of Siegert relation which follows;

$$g^{(2)}(q,t) = \frac{I(q,t) \cdot I(q,0)}{I(q,0)^2} = 1 + \beta g^{(1)}(q,t)^2$$

The angular brackets indicate the time average, I corresponds to scattered intensity, $g^{(1)}(q,t)$ corresponds to normalized electric field autocorrelation function and β is correction factor. The first order autocorrelation function is assumed as single exponential decay in order to derive diffusion coefficient (D) which is presented in Stokes-Einstein equation.

$$g^{(1)}(q,t) = \exp -\Gamma t$$

where Γ is a decay rate. As mentioned before hydrodynamic diameter of particles are calculated by diffusion coefficient (D) depending on wave vector (q) and decay rate (Γ) given below;

$$\Gamma = q^2 D$$

with,

$$q = \frac{4\pi\eta}{\lambda} \sin \frac{\theta}{2}$$

where λ is the incident laser wavelength, η is the refractive index of the sample and θ is the angle at which detector is located with respect to sample cell.

In this thesis, Malvern Zetasizer Nano S DLS instrument was used. A 633 nm red laser illuminates the solution and a detector measures the intensity of the scattered light at an angle of 173° [50]. The duration of each measurement was 10 seconds and up to 500 measurements were obtained. Since toluene was the dispersant, viscosity of toluene used in the particle size calculations. The hydrodynamic diameter of particles was determined according to intensity distribution. In cases that the samples had polydisperse size distribution, all particles sizes were taken into account during analysis if their contribution to total intensity was more than 10%. The detectable size range of the instrument is 0.6 nm-6000nm. 1.0-1.5 ml of homogeneous solution at 70°C was put in a glass cuvette and placed into the cell holder of the instrument kept at 26°C. The gelation was highly sensitive to the temperature. 26°C was determined as the optimum temperature for DLS measurements. At lower temperatures, the size of the aggregates grew so fast and went above the maximum measurable size of 6 μm . At higher temperatures, significant change in the aggregate size could not be observed within practical time intervals.

2.3 Ultraviolet-Visible Absorption Spectroscopy

Ultraviolet-Visible Absorption Spectroscopy (UV-Vis) is a technique in which the absorbed intensity of the light in UV-Visible spectral region (200-800 nm) was measured as it goes through the material. In the UV-Visible range, the molecules absorb light and undergo electronic transitions to higher energy levels. PBLG does not have any significant absorption band in UV-Vis (Figure 2.1). We have instead used UV-Vis

Absorption Spectroscopy as a measure of aggregation and turbidity in the solutions. As aggregates form in the solution and the solution gets turbid, the incoming light (intensity I_0) is scattered more and the intensity of light reaching the detector (I) will be less:

$$\% \text{ Transmittance} = I / I_0 \quad \text{Absorbance} = \log (I_0/I)$$

Though we still use the terms transmittance and absorbance, it is important to note that the absorbance is due to scattered light in the case of PBLG organogels.

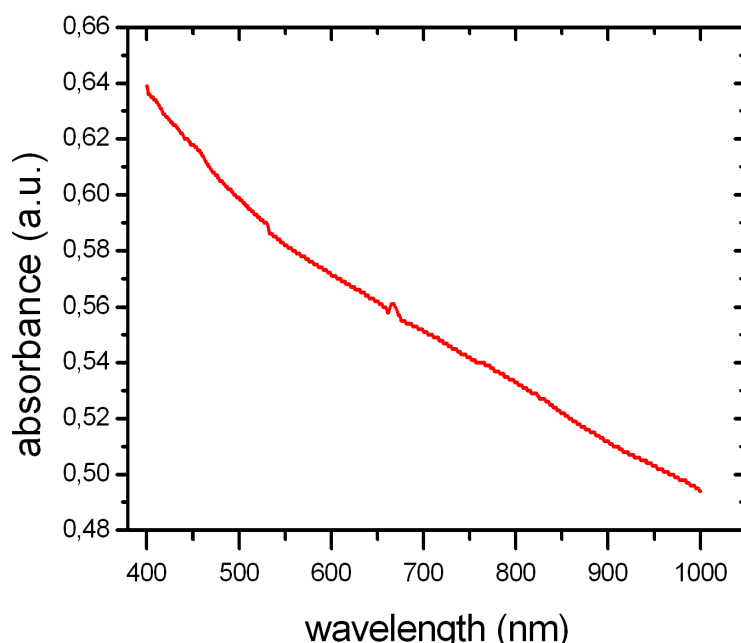


Figure 2.1 UV-Visible Spectrum of PBLG/toluene solution

UV-Vis spectra of PBLG gels were recorded by PG T80 UV/Vis Spectrometer. The instrument has two light sources: a tungsten lamp for visible region ranging between 300-1100 nm and a deuterium lamp for ultraviolet region between 190 to 400 nm. The sample holder was cooled by water circulation through Peltier temperature controller.

UV-Vis measurements were carried out at 23°C, 24°, 25° and 26°C. Concentration dependence of the solutions was analyzed at 23°C. Before each measurement, background was taken with toluene. Then, the homogeneous solution at 70°C was put into quartz cuvette (path length = 1 cm). The cuvette was placed in the sample holder of the instrument kept at temperatures mentioned above and the measurement was started immediately. For each sample, approximately 30 spectra were recorded consecutively.

2.4 Viscosity Measurements

Viscosity is a material property of the fluids and simply defined as the resistance of a fluid against flow. In a fluid, shear stress is proportional to shear rate and viscosity of the fluid is the proportionality constant,

$$\eta = \frac{\tau}{\dot{\gamma}}$$

where η is the viscosity, τ is the shear stress and $\dot{\gamma}$ is the shear rate. Fluids that show a linear relationship between shear stress and shear rate are called Newtonian Fluids. On the other hand if viscosity of fluids depend on the applied shear stress or shear rate, they are called Non-Newtonian fluids.

As the PBLG molecules restructure and aggregate at lower temperatures, the viscosity of the PBLG solutions increases in time. In this study, we have measured the viscosity using ANTON PAAR AMVn micro-viscometer. A spherical steel ball with a density of 7.85 mg/ml was used for analyzing dynamic viscosities of PBLG gels as a function of time. The optimum temperature for viscosity measurements was determined as 26°C in order to avoid spontaneous gelation which could block the ball's movement in the capillary. The viscosity was determined by measuring the time that a falling ball spends between two marks in an inclined capillary column. [51] . The inclination angle of the capillary could be changed. In the present study, the measurements were done at an angle of 30°. Depending on the concentration of the solutions and the resulting viscosity

values, different capillary sizes (and different ball sizes) were used. 50 measurements were taken in time at constant temperature.

The homogeneous PBLG solution at 70°C was filled into the capillary and the capillary was allowed to equilibrate in oven at 70°C for half an hour. The capillary was then taken from the oven, placed in the instrument in which the temperature of the capillary holder was set to 26°C. Viscosity measurements were carried out at PBLG concentrations of 0.4, 1.0, 3.0 and 5.0 mg/ml at 26°C. The smallest capillary with 1.0 mm diameter (viscosity range ~2-20 mPa.s) was used for the lowest concentrations of 0.4 and 1.0 mg/ml. 3 and 5 mg/ml PBLG solutions required a capillary having 1.8 mm diameter (viscosity range ~2.5-70 mPa.s).

The dynamic viscosities of the PBLG gels was calculated by device using the calibration constant $K_1(\alpha)$ of the measuring system, the rolling time t_1 and the difference in density $\Delta\rho$ between the ball and the sample [51].

$$\eta = K_1 \alpha * t_1 * (\rho_K - \rho_S)$$

where η is dynamic viscosity of sample [mPa.s], $K_1(\alpha)$ is measuring system calibration constant [mPa.cm³/g], t_1 is rolling time, ρ_K is ball density [g/cm³] (steel ball= 7.85 g/cm³) and ρ_S is density of sample to be measured (g/cm³).

2.5 Infrared Spectroscopy

Infrared (IR) spectroscopy was used to probe any structural changes of the PBLG molecules in solution in the wavenumber range of 100-5000 cm⁻¹.

Nicolet is10 FTIR Spectrometer was used at room temperature (~24⁰C) with a set up consisting of Mid-infrared Ever-Glo (9600-50 cm⁻¹) and Tungsten/halogen as light source, deuterated triglycine sulfate (DTGS) and liquid-nitrogen-cooled mercury cadmium telluride (MCT) as detector and diamond ATR as a sample holder. Before

taking measurement, background was recorded to eliminate the humidity and CO₂ contributions from air. The dried sample from 5 mg/ml PBLG gel was placed onto the ATR cell and the spectrum was taken at room temperature (~24°C). Spectrum was collected at 4 cm⁻¹ resolution using 16 scans.

2.6 Optical Microscope

A Leica DMLM optical microscope was used to observe structured PBLG network. The films were prepared by spin coating. ~ 200 µl of a homogeneous solution was taken by a micropipette, dropped onto a glass slide and then spin coated at 2000 rpm for 1 min to observe aggregate domains under microscope. Further observations were done with PBLG gel obtained by drop casting on a glass slide at room temperature to observe crystalline structure of gels under polarized light.

To observe crystalline structure of PS-PBLG gels, dried PS-PBLG gel obtained by evaporating toluene at room temperature was investigated by illumination of polarized light.

2.7 Differential Scanning Calorimetry (DSC)

Calorimetry is used to detect any heat generation or consumption during a chemical reaction or phase transitions. The determination of exchange heat via DSC is based on measuring difference of heat flow rate between sample and reference while they are subjected to controlled temperature [52]. When sample undergoes a physical transformation, its temperature begins to deviate from reference temperature. The device detects it and reduces the heat input to one cell while adding heat to the other, so as to maintain sample and reference at the same temperature. Consequently, mentioned temperature alteration between sample and reference corresponds to non-zero heat flow which forms the DSC signal.

The gel formation and melting were detected by DSC using TA Q200 Instrument. The cooling and heating rate was chosen as 5°C/min. The measurements were done under nitrogen flow. Gels were prepared from 10 mg/ml PBLG solutions by heating at 70°C for 2 hours and then cooling at 23°C. 8 mg of the gel was weighed into an Aluminum Hermetic Pan and the pan was sealed. An empty sealed aluminum pan was used as reference for the measurement. Measurements were carried out between 0°C and 70°C.

2.8 Atomic Force Microscopy (AFM)

AFM is a technique in which the interaction force between sample surface and a sharp probing tip is monitored to display the surface morphology. AFM measurements have high vertical resolution on the order of fractions of nanometer. Thus atomic-scale defects, molecular structures and perfectly ordered atomic structures can be observed via AFM. It consists of a cantilever having probe at its end, a sharp tip, a piezoelectric cylinder, laser and a photodiode detector. The main types of imaging modes are; contact mode, non-contact mode and tapping mode. The working principle is based on measurement of deflection of the cantilevers. Surface structure is obtained from the alteration of vibration amplitude of the cantilever.

AFM experiments were carried out at room temperature in air using NT-MDT Solver P47 instrument. 200 µl hot solutions of 0.4 mg/ml PBLG/toluene and 1 mg/ml PBLG-PS/toluene at 70°C were dropped onto glass slides, allowed to cool at room temperature for ~15 min and then spin coated at 2000 rpm for 1 min. Tapping mode was used for imaging the morphology of the samples.

Chapter 3 PBLG/toluene Gels

3.1 Motivation

Poly (γ -benzyl-L-glutamate) (PBLG) is a synthetic polypeptide which forms α -helical secondary structure in most organic solvents. Therefore, it has been investigated as a model rigid rod polymer in a variety of organic solvents, especially to understand the gelation of rigid rod molecules. Favorable interactions between the solvent and side chain benzyl groups of α -helical PBLG play a key role in its solubility at temperatures above $\sim 50^{\circ}\text{C}$. Due to change in interaction strength with temperature, PBLG-solvent system undergoes a transition from solution to gel as the temperature is decreased. Aggregation of PBLG only occurs in solvents which do not disrupt helical conformation of PBLG [30] therefore it is important to use helicogenic solvents such as benzene, benzyl alcohol, toluene etc. in order to investigate gelation phenomenon.

The gelation of PBLG, in particular the structure formation during sol-gel transition, greatly depends on temperature, concentration and time. The factors affecting reversible gelation of PBLG have been previously investigated [24, 36, 41]. Moreover, the nature of phase transition and the properties of the PBLG solutions in different phases have been discussed [36, 43, 46]. Various mechanisms were considered in the literature to explain the thermoreversible gelation PBLG solutions [40-42] as discussed in Chapter 1. Still, a general understanding of structure formation, mechanism and kinetics of gelation of PBLG-solvent system could not be reached. To explore the thermoreversible gelation of rod-like molecules further, we studied the gelation of PBLG in toluene as a model system. The results of gelation of PBLG in toluene as a function of temperature, concentration and time will be presented in this chapter. Different stages of structure formation and aggregation in the solution during gelation were monitored by DLS, UV-Vis Spectroscopy, viscosity measurements and DSC.

3.2 Results&Discussion

3.2.1 Determination of Critical Concentration and Temperature for Gelation

Critical Gelation Temperature (T_{gel}): In this thesis, critical gelation temperature for a given concentration of PBLG solution in toluene corresponds to the temperature below which a macroscopic gel is formed that does not flow against gravity. PBLG solution in toluene cannot form a macroscopic gel above this temperature, but behaves as a viscous fluid consisting of gel-like aggregates. Above T_{gel} PBLG still self-assembles in toluene into aggregates consisting of network structure. The viscosity of the solution increases due to aggregate formation, but the aggregates cannot form a single interconnected network that can be considered as a solid-like material. Micron-sized coagulates cannot entrap toluene molecules completely and the system behaves like a viscous fluid rather than a soft solid (gel) with a yield point.

Determination of the critical gelation temperature is important as the effect of some other factors on gelation such as concentration and additives can be followed as a shift in T_{gel} . T_{gel} was determined as described in Chp. 2.

Figure 3.1 shows the pictures of PBLG-toluene samples in vials which were turned upside down after keeping the homogeneous solutions at different temperatures for 2 h. Fig. 3.1 (a) and Fig. 3.1 (b) correspond to the samples kept at 30°C and 28.5°C, respectively. Both solutions flowed down indicating that a macroscopic PBLG-toluene gel did not form. As homogeneous PBLG-toluene solution was cooled down to 26°C, aggregates appeared in the solution. Although PBLG molecules could assemble at 26°C as visible aggregates, system did not undergo macroscopic gelation. The aggregates remained suspended in the solution without attaching to each other. As a result, sample moved against gravity when the vial was inverted (see in Figure 3.1 (c)). On the contrary, when the solution was cooled down 23°C, system achieved to form 3D

network which could immobilize toluene. Macroscopic gel was observed as shown in Figure 3.1(d).

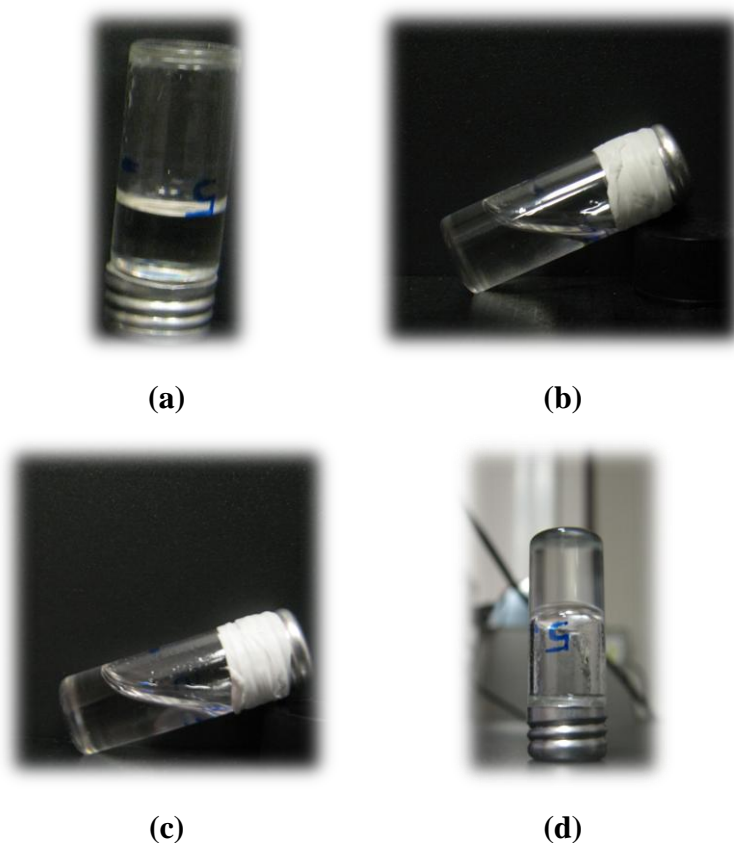


Figure 3.1 5.0 mg/ml PBLG in toluene was cooled down from 70 °C to (a) 30 °C, (b) 28,5 °C, (c) 26 °C and (d) 23 °C. The solutions were kept at specified temperatures for 2 h and then the vials were turned upside down. Only in (d) a macroscopic gel was formed which did not flow down against gravity.

The sample kept at 23 °C was cloudy and did not move when slightly tilted. It was not possible to distinguish two distinct phases (PBLG aggregates suspended in toluene) as in the sample of Fig. 3.1 (c). When the vial was turned upside down, the sampled did not flow down indicating the presence of stable macroscopic gel. Based on these visual observations, we conclude that the critical gelation temperature for 5 mg/ml PBLG solutions in toluene is between 23 °C and 26 °C. Although this is a wide temperature

range and quite rough to assign as T_{gel} , it helped us to design the other experiments for further investigations. A more accurate determination of T_{gel} by DSC will be later introduced in this chapter.

Critical Concentration: Critical concentration (C^*) is the smallest concentration of PBLG in toluene which formed a macroscopic gel at 23°C. Since 5.0 mg/ml PBLG in toluene was known to form gel at 23°C (Fig. 3.1 (d)), critical concentration was expected to be lower than 5.0 mg/ml. Homogenized solutions having concentrations of 1.0, 2.0, 3.0, 4.0 and 5.0 mg/ml of PBLG in toluene were kept at 23°C for 2 h. Fig. 3.2 shows the pictures after the vials were turned upside down.

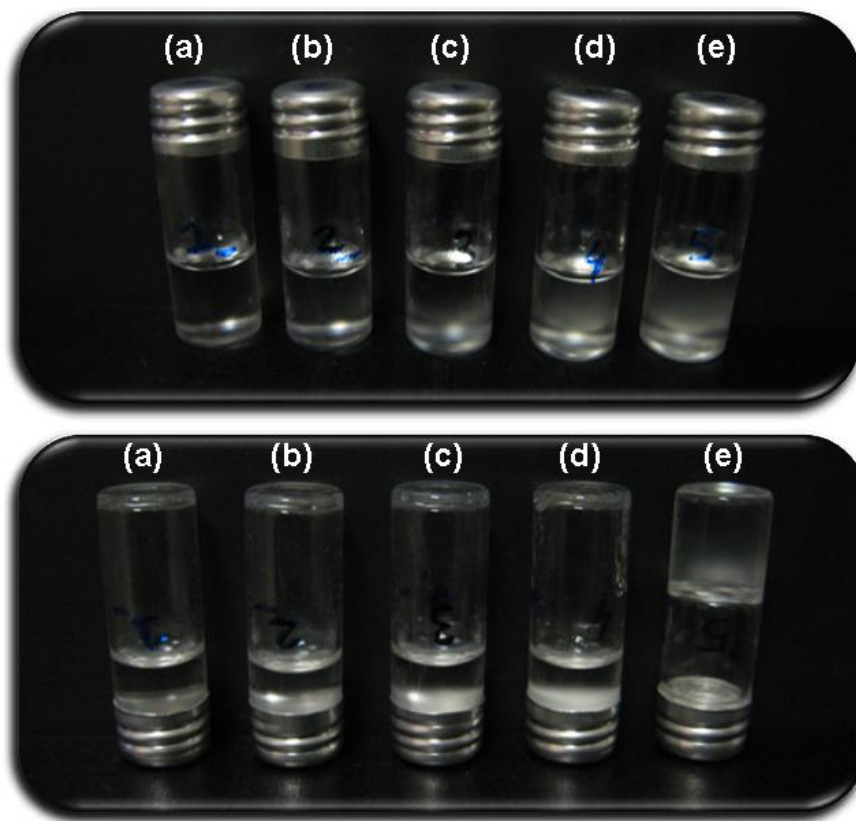


Figure 3.2 Homogeneous PBLG-toluene solutions having concentrations of 1.0 mg/ml (a), 2.0 mg/ml (b), 3.0 mg/ml (c), 4.0 mg/ml (d) and 5.0 mg/ml (e) respectively. The solutions were kept at 23°C for 2 h and then the samples were subjected to gravity. Only in (d) macroscopic gel was formed which did not flow down against gravity.

For 5 mg/ml solutions the gel formed at 23°C did not flow down under gravity. Weak gel was obtained from 4.0 mg/ml solutions which can be destroyed spontaneously by gravity. No macroscopic gel formation was observed in other solutions. Based on these visual observations, we conclude that the critical concentration C^* for PBLG (MW 30,000-70,000 g/mol) in toluene at 23°C is between 4.0 mg/ml and 5.0 mg/ml. For PBLG-toluene system, Tipton et al. reported C^* for lower molecular weight of PBLG (16,000 g/mol) as 0.494 ± 0.32 (w/w %) based on DSC results [36]. They suggested that concentration of PBLG in toluene should be higher than 0.494 ± 0.32 (w/w %) in order to form gel because enthalpy of melting is zero at that concentration. This corresponds to a concentration of 4.2 mg/ml which is consistent with our observations despite the molecular weight difference. Since chain length is effective on gelation [48], our result for C^* is reasonable considering increase in molecular weight. One further point is C^* can also vary depending on temperature which solution is cooled down. If the solution of PBLG-toluene is cooled down from 70°C to higher temperatures than 23°C, C^* will be expected to be higher

3.2.2 Determination of critical temperatures by DSC

A more accurate determination of the critical temperatures both for gelation and for gel melting was done by DSC. 10 mg/ml PBLG gel was prepared by cooling hot solution to 23°C and then put in DSC to be able to observe the melting peak. A ramp of 5°C/min was performed in order to measure the endothermic and exothermic peaks. Figure 3.3 shows the DSC heating and cooling curves for the gel prepared from 10 mg/ml PBLG-toluene.

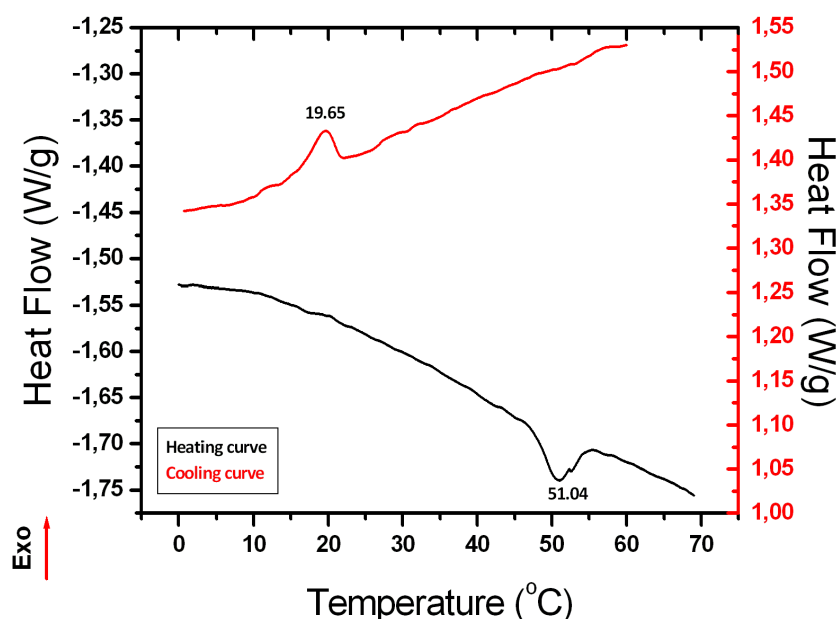


Figure 3.3 Heating and cooling DSC cycles of 10 mg/ml PBLG-toluene solution. Exothermic peak at 19.65°C corresponds to gelation of PBLG-toluene solution and endothermic peak at 51.04°C corresponds to melting of PBLG gel. Scan rate was 5°C/min.

Gel melting and gelation peaks were clearly seen at 51.04°C and 19.65°C, respectively. It should be noted that in between cooling and heating process, sample was annealed at 70°C and 0°C for 15 min to avoid inhomogenities. This might have caused evaporation of toluene and a change in the concentration. Still, the observed gelation temperature of 19.65°C at a cooling rate of 5°C/min is consistent with the 23°-26°C obtained in visual observations. Tipton et al. proposed that the endothermic peak in the heating curve was an evidence of the interaction between the PBLG molecules in toluene [36]. The melting temperature they obtained from endothermic peaks observed in DSC for PBLG-toluene gel varied between 38-41°C. Our result for melting temperature (51.04°C) is significantly higher than Tipton et al.'s result which might be attributed to the use PBLG having different molecular weight and concentration. As mentioned in Section 3.2.1, we have used higher molecular weight of PBLG which possess longer chains with more benzyl side groups. Since interactions governing the gelation are assumed to

be π - π stacking, increase in number of aromatic moieties can make the system more robust resulting with a shift in melting towards higher temperatures.

To check further whether the gels formed can maintain their form at 50°C, we have observed the gel in an upside down vial as the temperature was increased.

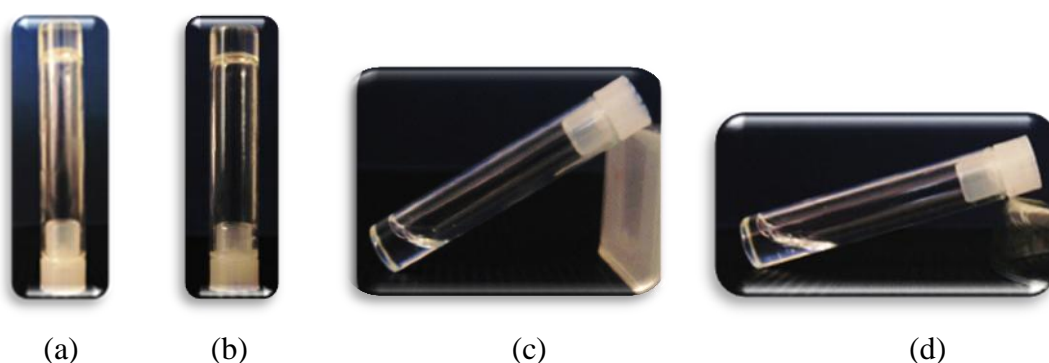


Figure 3.4 Optical photos of 5 mg/ml PBLG-toluene gels which were kept at (a) 23°C, (b) 30 , (c) 50°C and (d) 70°C for 2 h. In (a) and (b) macroscopic gels did not move down against gravity. (c) corresponds to viscous fluid which lost its stability and (d) corresponds to homogenous PBLG solution.

Gels were formed from 5 mg/ml PBLG-toluene by waiting 2 hours at 23°C. Figure 3.4 shows the pictures of the gels in upside down vials at different temperatures. The gel lost its stability at 50°C after 2 h of waiting time which is in good agreement with our DSC result. At 70°C, gel was completely melted and turned into a homogeneous solution.

3.2.3 Gelation Kinetics as Observed by DLS Measurements

Behavior of PBLG gels as a function of time has been studied extensively by Dynamic Light Scattering [53]. With decreasing temperature, intermolecular interactions arise between PBLG helices by means of benzyl side groups [46]. The assembly of PBLG molecules gives rise to form bundles and fibers resulting in aggregation during cooling process. The aggregation process of PBLG in various solvents has been widely studied

as a function of time and temperature [41, 42, 53]. In this respect, DLS technique can be employed to understand the aggregation process of PBLG-toluene solutions over time while temperature was set constant close to T_{gel} .

Previous literature related with dynamic light scattering studies of PBLG gels were generally based on measuring intensity or autocorrelation function as a function of time [46], temperature [42] and concentration [36]. For instance, utilization of correlation function in order to determine gelation time was done by Shukla [46]. His research was based on understanding gelation in PBLG-benzyl alcohol system by working at different temperatures. He explained the gelation temperature considering autocorrelation function. In detail, he argued that if the set temperature was close to gelation temperature, autocorrelation function showed a damped oscillatory decay. In this regard, he assigned gel point as 32°C where he monitored an oscillatory decay over time.

To understand the structure formation during gelation of PBGL-toluene system, we have monitored the time dependence of aggregate size at different concentrations and temperatures. Since DLS measurements depend on the diffusion of the aggregates in the solution, we have chosen the measurement temperature as 26°C which is at the upper end of the gelation temperature. At lower temperatures, aggregates grow quite fast above the DLS detection limit ($\sim 6 \mu\text{m}$) and the gel state is reached where diffusion of aggregates is not possible. PBLG-toluene samples at concentrations of 0.4, 1.0, 3.0 and 5.0 mg/ml were used for the measurements at 26°C. At 26°C for higher concentrations, DLS measurements also suffered from too fast growth of aggregates similar to lower temperatures.

PBLG-toluene solutions were homogenized at 70°C in oven and then placed into the Dynamic Light Scattering instrument where the sample cell temperature was set constant at 26°C. 500 measurements were carried out, each at 10 second run time.

Hydrodynamic diameters of aggregates were obtained from intensity correlations using toluene viscosity as the medium viscosity. The size distributions were not unimodal as expected, and the size of the second and third peaks, where present, were also recorded.

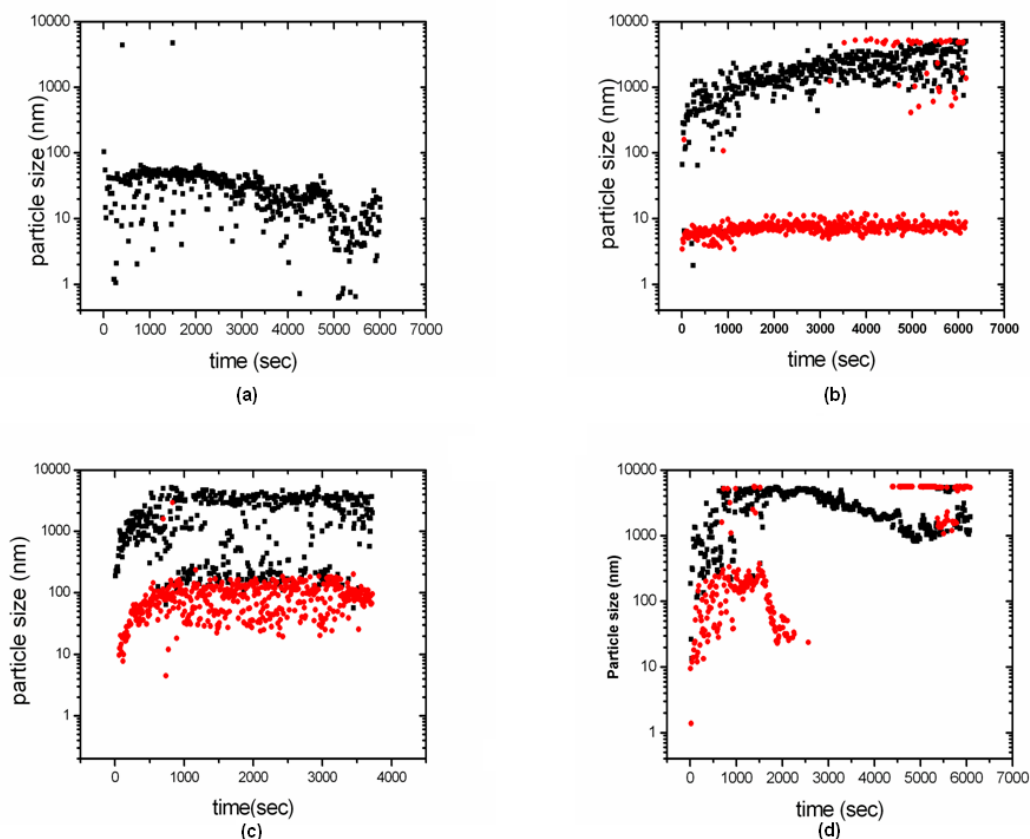


Figure 3.5 Aggregate size growth as a function of time measured for homogeneous PBLG- toluene solutions having concentrations of (a) 0.4 mg/ml, (b) 1.0 mg/ml, (c) 3.0 mg/ml and (d) 5.0 mg/ml recorded at 26°C. The size of first peak is represented by (■) and second peak is represented by (●)

Figure 3.5 shows the change in aggregate size as a function of time for the four different PBLG-toluene samples. The aggregation of PBLG-toluene samples depended significantly on time. For 0.4 mg/ml PBLG/toluene solution, aggregate size did not change over time. On the contrary, for solutions with a concentration of 1.0, 3.0 and 5.0 mg/ml aggregates grow larger over time. Time required to reach aggregate size of 5000 nm was more than 5000 seconds for 1.0 mg/ml, ~600 sec for 3.0 mg/ml and ~500

seconds for 5.0 mg/ml PBLG solutions. It is noteworthy that the decrease in aggregate size was observed first in smaller size aggregates then in larger size aggregates for 5 mg/ml PBLG/toluene solutions after 1000 seconds (Figure 3.5 (d)).

The evolution of aggregates with time indicates that gelation is significantly depends on time. Elapsed time until aggregate size reached a constant value corresponds to formation of aggregates from PBLG bundles. Considering the steady state behavior of 0.4 mg/ml PBLG/toluene solution over time, we interpret that fundamental fibers are formed at elevated temperatures therefore formation stage of 0.4 mg/ml PBLG solution occurs too fast to detect by DLS. As concentration increases towards C^* , the growth was remarkably faster compared to lower concentration samples. It can be explained by increase in interactions between PBLG helices which accelerates assembly of smaller aggregates. Since 5.0 mg/ml PBLG-toluene sample which had concentration larger than C^* (Figure 3.5 (d)) formed a stable macroscopic gel, the aggregate size grew very fast. The decrease in the size of smaller aggregates can be interpreted as the attachment of smaller aggregates to larger aggregates. The decrease in the larger aggregate size after ~2500 seconds may indicate the precipitation of the growing aggregates in the sample.

For 0.4 mg/ml PBLG-toluene aggregate size stayed constant between 10-100 nm but it did not grow larger (Fig. 3.5 (a)). For 1.0 mg/ml PBLG-toluene, two different aggregate sizes were observed. The sizes of the smaller aggregates stayed constant in the range of 1-10 nm. But, the larger aggregates grew in size from ~100 nm to ~3000 nm and nearly stayed constant around that value (Figure 3.5 (b)). The data of 1 mg/ml PBLG-toluene sample confirmed the structuring of PBLG even at concentrations below C^* . The time dependence of aggregate formation for 3 mg/ml PBLG-toluene sample is shown in Figure 3.5 (c). Similar to 1 mg/ml PBLG-toluene sample two different aggregate sizes were observed. Both sizes grew in time from 10 nm to 100 nm for smaller aggregates and from 100 nm to 5000 nm for larger aggregates. Figure 3.5 (d), shows aggregate

growth of 5 mg/ml PBLG-toluene sample. Second size peak almost disappears in 2000 seconds due to exhibiting unimodal behavior.

From Figure 3.5 it can be seen that growth rate increases with increasing PBLG concentration in toluene. We identify 0.4 mg/ml PBLG-toluene solution at which aggregate size was the minimum. This can be understood considering the dilute concentration of the solution. Since the concentration is much smaller than C^* , a single macroscopic 3D network cannot be formed. A single PBLG α -helix (for MW 30000-70000) is expected having a contour length in the range of 19-45 nm (according to our estimation based on assuming a single residue having a length of 0.150 nm [54]) and width of ~ 2 nm [54]. In this respect, measured sizes of PBLG, even for 0.4 mg/ml PBLG solution, are above dimensions of a single PBLG helix. This indicates that DLS data is consistent with structuring of PBLG in toluene even at low concentrations. As shown in Figure 3.5 (b), measured particle size starts to exhibit obvious increase with increasing concentration (1.0 mg/ml PBLG-toluene). This aggregate size increase is due to association of small clusters of PBLG with elapsed time. Even at a concentration of 1.0 mg/ml PBLG-toluene lower than C^* a significant aggregate growth is observed from 100 nm to 3000 nm. Growth of aggregates could be an evidence for reduction of diffusion coefficient (D) regarding Stokes-Einstein equation possibly due to entanglement interactions between PBLG chains with increasing concentration [53]. It should be noted that small aggregates were not consumed completely during formation of larger aggregates in 1.0 mg/ml PBLG-toluene solution. This suggests that system does not form a gel at this concentration because gelation requires a continuous network in which a single aggregate is expected. With a further increase in concentration as given in Figure 3.5 (c), drastic change was observed in the second peak. The growth of small aggregates could be explained by reduction of distance between PBLG aggregates with increasing concentration which facilitates attractive intermolecular forces between clusters. In addition, growth rate of particles increases with concentration because the formation of PBLG is faster. On the contrary, concentration of 5 mg/ml PBLG-toluene

solution represents a transient rod-like polymer network formed at 26°C. Since macroscopic gelation does not occur for 5 mg/ml PBLG-toluene sample at 26°C, obtained DLS result shows pregel state in which aggregated PBLG molecules weakly attach to each other. This indicates that even small domains of PBLG molecules grow to construct a continuous network.

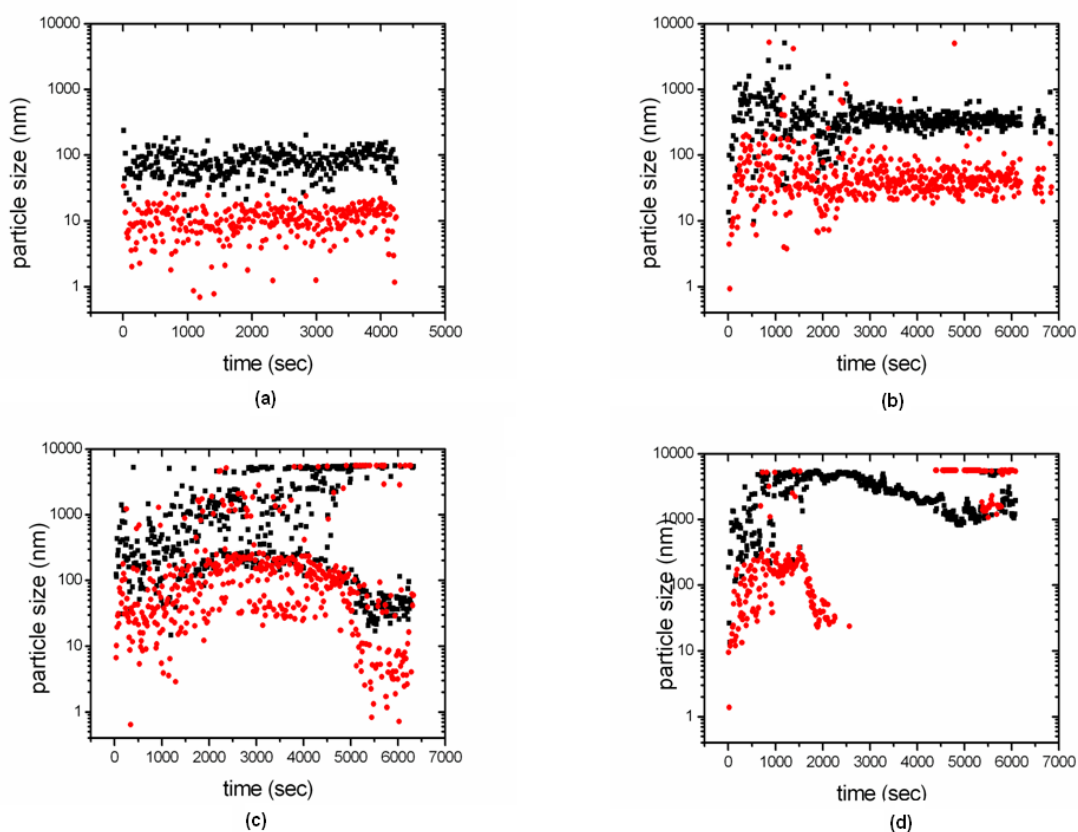


Figure 3.6 Aggregate size growth as a function of time measured for homogeneous PBLG- toluene solutions having concentration of 5.0 mg/ml recorded at (a) 30°C, (b) 28.5°C, (c) 27°C and (d) 26°C. The size of first peak is represented by (■) and second peak is represented by (●).

Gelation kinetics of 5 mg/ml PBLG-toluene solutions was examined at different temperatures. Although temperature varies in a short range of 26°C-30°C, size of aggregated PBLG chains changes significantly. When the PBLG-toluene solution was allowed to cool slowly from 70° to 30°C, aggregate size was detected at 10 nm and 200 nm. As mentioned, single PBLG chain has a length of ~45 maximum and width of 0.15

nm whereas measured size of PBLG molecules at 30°C was significantly higher. This indicates that DLS data collected at 30°C belongs to aggregated PBLG molecules. As shown in Figure 3.6 (a), hydrodynamic diameter of PBLG aggregates do not grow over time. PBLG may aggregate at higher temperatures [36] therefore we could not achieve to monitor growth stage at 30°C. When the temperature was changed by 1.5°C, we observed fluctuations in aggregate size during 2000 seconds which can be explained by competition between thermal energy and attractive intermolecular forces. When the temperature decreases, thermal energy driving the separation of structured PBLG chains decreased and intermolecular interactions becomes dominant [46]. Also, increase in aggregate size could be an evidence for interconnection of small PBLG domains with decreasing temperature. By approaching gelation point, we observed a tremendous fluctuation in particle size (Figure 3.6 (c)). The highly scattered data taken at 27°C could be an evidence for enhancing the intermolecular interactions between PBLG domains. The fluctuated DLS data arises from significant changes in the scattered intensity over time. Interestingly, this behavior appears with a decrease in temperature of 1.5 °C and it emphasizes the high sensitivity of gelation to temperature. Shukla et al. and Oikawa et al. have also reported an apparent fluctuating decay in autocorrelation functions, which is also related with scattered intensity, of PBLG solutions near gelation threshold [46, 53]. Shukla et al. related the oscillatory decay of autocorrelation with onset of gelation and they determined gelation temperature at which they observed this behavior [46]. The fluctuations on scattered intensity could be interpreted that PBLG aggregates coupled strongly near gelation threshold and caused a continuous reduction of energy in time resulting with underdamped oscillatory behavior [53]. On entering the gel phase given in Figure 3.6 (d), we observed a growth in size with time indicating the formation of interconnected fibrillar network. Because of the strong scattering intensity of PBLG molecules, measured aggregate size increased in time until it reaches a maximum of 5000 nm. According to Shukla et al. growth of aggregates over time cannot be explained through spinodal decomposition mechanism [46]. Therefore

another mechanism should be considered in order to explain gelation of PBLG-toluene systems.

3.2.4 Viscosity Measurements

Gelation kinetics of PBLG is strongly affected by concentration as explained in Section 3.2.3. At the concentrations above C^* aggregates of PBLG exhibit drastic increase in size with higher growth rate compared to low concentrations. The growth of aggregates is expected to cause an increase in viscosity during gelation and go to infinity as a non-flowing macroscopic gel is formed. Since viscosity of PBLG gels are time dependent, kinetics of gelation can be studied by analyzing change in viscosity with time.

Very few investigations were reported on measuring viscosity to follow gelation kinetics of PBLG solutions. Murthy et al. reported effect of time on dynamic mechanical properties of PBLG-benzyl alcohol solution based on complex viscosity results [55]. Their result showed that complex viscosity of PBLG-benzyl alcohol solution increased in 3 h.

The same temperature of 26°C, as in DLS measurements, was chosen for viscosity measurements to be able to observe gelation kinetics over large time intervals. At lower temperatures, gelation was fast and the falling ball viscometer could not be used for more than couple of minutes. Increase in viscosity was examined during gelation of PBLG solutions at different concentrations of 0.4, 1.0, 3.0 and 5.0 mg/ml. Growth of aggregates limit taking further measurements with time similar to lower temperatures.

Homogenous PBLG-toluene solutions were filled into capillary and then placed in capillary holder where the temperature was kept constant at 26°C. The horizontal angle of the capillary was set to 30°. Growth of PBLG clusters are growing over time without encountering any restrictions (i.e. insufficient PBLG, fluctuation of temperature) until the ball is immobilized into the capillary due to formation of solid-

like material. This run was used for assigning as the time for gelation at 26°C concerning viscometer instrument.

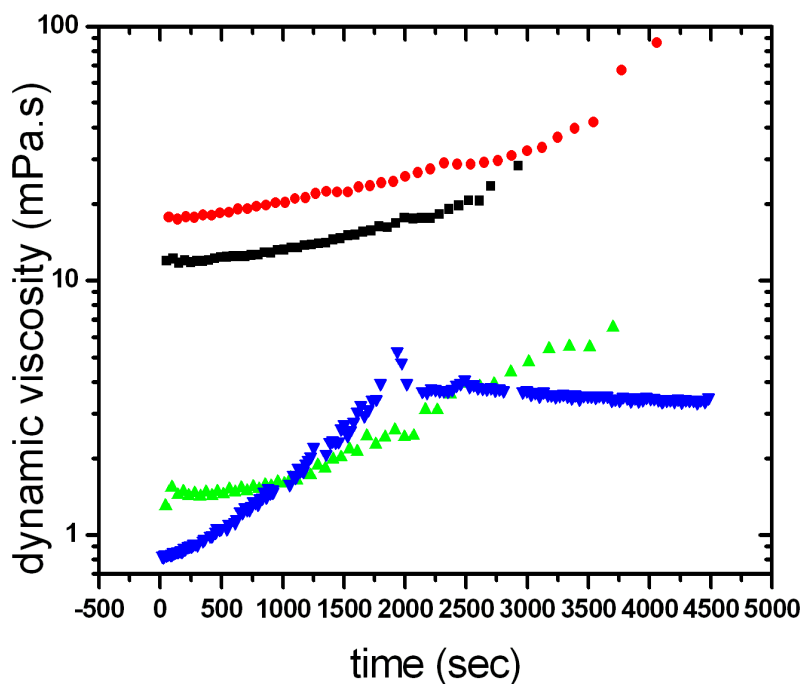


Figure 3.7 Time dependency of viscosities of 0.4 mg/ml (\blacktriangle), 1.0 mg/ml (\blacktriangle), 3 mg/ml (\blacksquare) and 5 mg/ml (\bullet) PBLG/toluene solutions at 26°C.

The change of dynamic viscosity in time is seen in Figure 3.7 for different PBLG concentrations in toluene. For 0.4 mg/ml PBLG-toluene sample, the viscosity increased in time and reached a plateau value. This plateau value was 4 mPa.s for 0.4 mg/ml sample. For 0.4 mg/ml sample, the observation of a peak viscosity at ~5.5 mPa.s and then decrease to a constant value of 4 mPa.s can be due to the disruption of the formed structures by the falling ball. The system can be said to reach a dynamic equilibrium in the case of a falling ball. Such a peak was not observed for 1.0 mg/ml sample. Increase in viscosity in ~ 3700 seconds clearly shows the structure formation in the solution towards gelation. Contrary to the observation of a plateau value in viscosity for low concentrations, the viscosity of 3 and 5 mg/ml PBLG-toluene samples increased

gradually. After 3000 seconds, both 3 mg/ml and 5 mg/ml sample had a viscosity of ~30 mPa.s. Viscosity of 5 mg/ml sample then increased further to 90 mPa.s. The viscosity data for all samples were recorded until the ball stuck in capillary. The reason to block the movement of ball is aggregated PBLG molecules. At the beginning stage of gelation, formation of aggregates caused increase in viscosity therefore the speed of ball reduced dramatically and it causes an increase in viscosity shown in Figure 3.7.

3.2.5 Turbidity Measurements by UV-Visible Spectrometer

UV-Visible spectroscopy is generally used for the quantitative determination of the concentration of organic compounds and transition metals in solutions. The species can also be identified from their characteristic absorbance peak in the UV-visible region. In addition, the presence of interactions between different species in a solution can be determined through the shifts of the absorption peaks. In the present study, we used UV-visible spectrometer to follow gelation kinetics by probing the change in the turbidity as reported in earlier studies [56]. As the PBLG molecules structure and the aggregate size increases during the gelation process, UV-Visible light is scattered strongly when the size of the aggregates (or the structural features) is of the order of the wavelength.

The appearance of PBLG-toluene gels vary from translucent to opaque depending on cooling conditions. In the present study, solutions were allowed to cool slowly therefore obtained gels were cloudy [36]. To investigate increase in turbidity of PBLG-toluene gels over time we used UV-Visible Spectrometer. Our results supported that 25 min could be enough for obtaining gel network from 5.0 mg/ml PBLG/toluene solution at 23°C. Different kinds of techniques which were used for determination of gelation time [27].

The same PBLG/toluene solution concentrations (0.4, 1.0, 3.0, 5.0 mg/ml) were chosen for the measurements. 30 spectra were taken consecutively in the wavelength range of

200-1100 nm after the homogenized hot solution was placed into the sample holder whose temperature was kept constant at 23-26°C. One spectrum took nearly 4 minutes. So the total time for the whole measurement was ~ 120 min. The measurement time was chosen long enough to observe the macroscopic gelation as indicated by the DLS, viscosity measurements and visual observations.

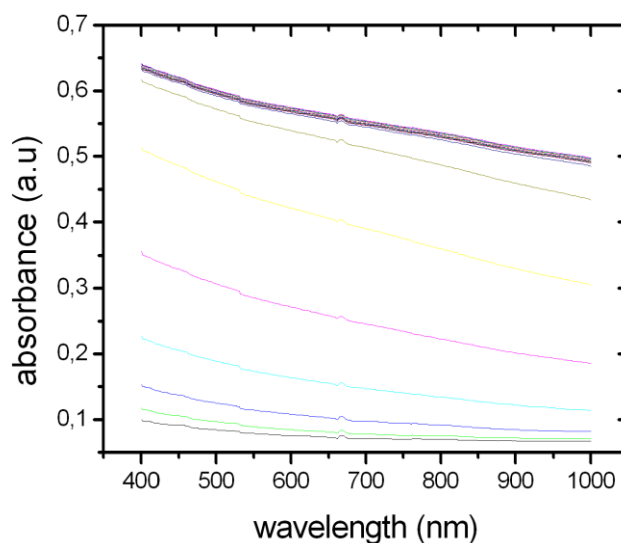


Figure 3.8 Time dependent evolution of the UV-Visible Spectra of 5.0 mg/ml PBLG/toluene solution recorded at 23°C over a 2 hour period.

The decrease in the transmittance (increase in absorbance) of UV-Visible light due to scattering by the self assembly of PBLG molecules into aggregates was monitored by UV-Visible Spectrometer in the wavelength range of 400-1000 nm at different times as shown in Figure 3.8 over time. Growth of aggregates causes remarkable increase in absorbance over a 2 h-period as expected. To analyze kinetics of gelation more precisely, absorbance change was plotted against time at a specified wavelength. Since PBLG does not show any characteristic absorbance peak in the range of 400-1100 nm

(see in Figure 3.8), 600 nm was chosen for the analysis. Similar results were obtained at other wavelengths as well.

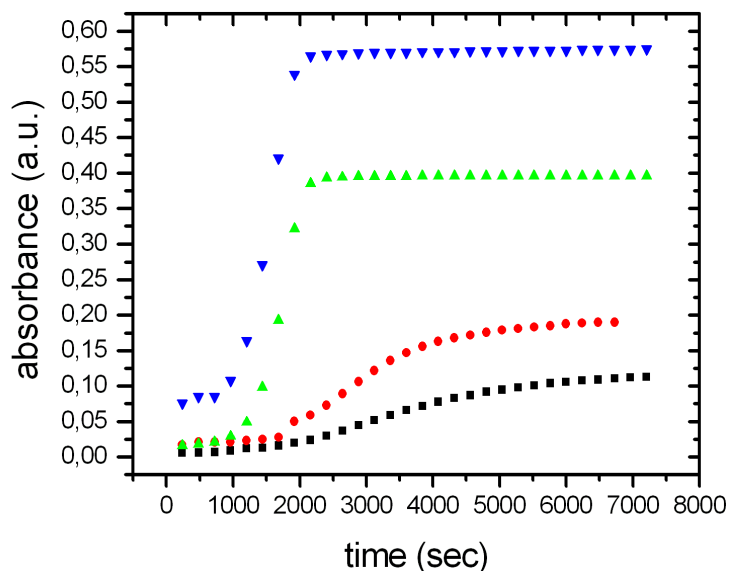


Figure 3.9 Turbidity curves showing aggregate formation of PBLG/toluene solutions having concentrations of 0.4 mg/ml (■), 1.0 mg/ml (●), 3.0 mg/ml (▲) and 5.0 mg/ml (▼) over time. Data were collected at 600 nm since cooling from 70°C to 23°C.

Figure 3.9 shows the effect of time on aggregation process of specified PBLG-toluene samples according to the absorbance change at 600 nm. Both the maximum value of the absorbance and its rate of change depend on the solution concentration. In attempt to determine the critical gelation time and absorbance change for each concentration, sigmoidal fit was applied to turbidity curves of PBLG solutions shown in Figure 3.10. Sigmoidal growth model can be used to describe a growth process which behaves exponentially at the beginning stage then slow down and stops at the end when the system becomes saturated. Generally, sigmoidal curves have been used for biological related studies. Also literature includes some reports on utilization of this type of curves to understand gelation kinetics [57, 58]. In PBLG-toluene solutions sigmoidal function

fits well to the time dependence of absorbance. In the analysis we have defined A_1 as the minimum absorbance of small aggregated PBLG molecules and A_2 as the maximum absorbance where the aggregate size remained constant. The inflection point (t_i) corresponds to critical gelation time where aggregation slows down and calculated from the intensity is at height/2 (Figure 3.10). ΔA shown in Figure 3.10 corresponds to growth phase presenting between the initial and final stage of gelation process. It should be noted that sigmoid curves of PBLG solutions strongly depend on concentration.

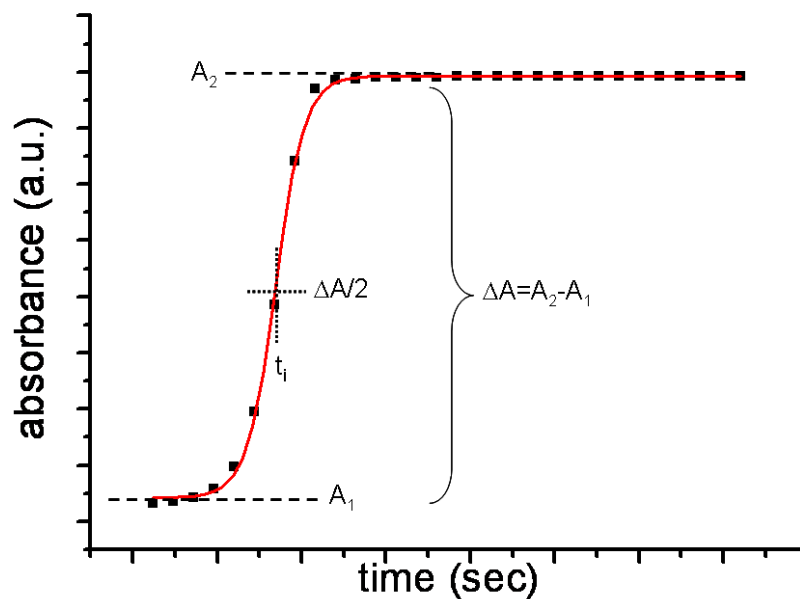


Figure 3.10 Determination of gelation time (t_i) and change in absorbance (ΔA) from sigmoidal fit to the UV-Vis data of Fig. 3.9.

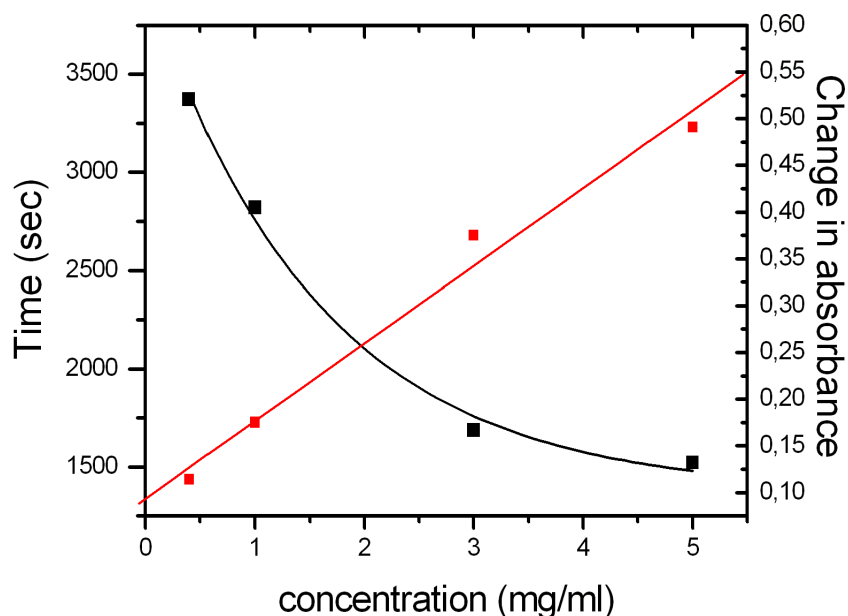


Figure 3.11 Critical time for gelation (■) and change in absorbance (■) as a function of PBLG/toluene concentration. Determination was done by applying sigmoid fit to specified concentrations as shown in Fig. 3.10.

The large increase in scattering during gelation was used to follow gelation kinetics of PBLG-toluene solutions. Figure 3.11 shows the change in absorbance (ΔA) and the critical gelation time as a function of the concentration of PBLG solutions. It can be clearly seen that the critical time decreases exponentially with increasing concentration. UV-Vis spectrometry indicates that most of the gel formation is completed within the first 25-60 min. At lower concentrations than C^* , critical gelation time for cluster-cluster aggregation is in the range of 3500- 2500 seconds. As concentration of PBLG-toluene increases above C^* , system reaches final state in 1700-1500 seconds. This may indicate that intermolecular interactions between neighboring PBLG molecules are facilitated by increasing concentration [53] therefore it takes less time for aggregated PBLG molecules to meet and attach each other towards forming a macroscopic gel . The most prominent sign of the gelation process is the increase in scattered intensity which is due to aggregation of PBLG molecules in toluene [42]. At the beginning of

gelation, scattered light stayed constant for a while indicating that UV-Visible Spectrometer is not sensitive to early stages of structuring where the aggregate sizes are less than 600 nm (see Figure 3.9). Thus, we attribute the increase in absorbance to the macroscopic gel formation. The previously formed PBLG structures that grew into large aggregates attach to each other and form a macroscopic gel. The evidence for this comes from UV-Vis data of 5 mg/ml sample measured at slightly higher T (26°C) where we did not see macroscopic gelation but we know from DLS that there are large (~ 5000 nm) aggregates.

Figure 3.11 provides information on change in absorbance (ΔA) of PBLG-toluene solutions with concentration. ΔA increases linearly with concentration indicating more structuring in concentrated solutions. For 0.4 mg/ml PBLG-toluene solution, aggregates do not grow remarkably over time (see Figure 3.9), which is in good agreement with DLS results therefore absorbance remains low resulting with small ΔA . We interpreted that the absence of continuous network in dilute concentrations restricts change in absorbance. With increase in concentration, ΔA increases which is due to association of small aggregates. ΔA reaches at maximum as expected considering 5 mg/ml PBLG-toluene solution, since non-flowing gel can be formed at this concentration.

The direct evidence shown in Figure 3.12 strongly suggests that increase in ΔA corresponds to attachment of aggregates and macroscopic gel formation. Figure 3.12 compares the absorbance as a function of time for 5 mg/ml PBLG solution at 23°C and at 26°C. At 26°C, a sudden increase in absorbance could not be observed within 5000 seconds. Although aggregates grew upon 5000 nm (see Section 3.2.3) and viscosity rapidly goes towards 90 mPa.s (see Section 3.2.4), UV-Visible spectrometer cannot detect any change in absorbance at this temperature. This may indicate that there is significant structuring but no attachment of aggregates to form a gel at 26°C as supported by our observations (see Section 3.2.3). We consider that formation of 3D

network is a result of associated aggregates and this process strikingly depends on temperature.

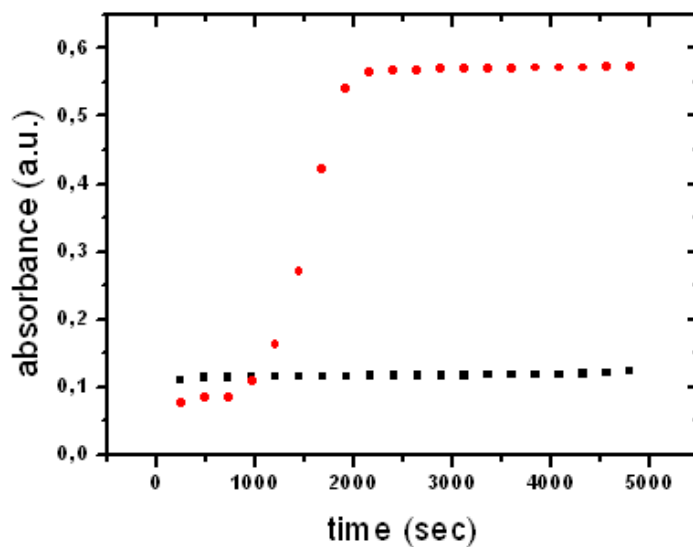
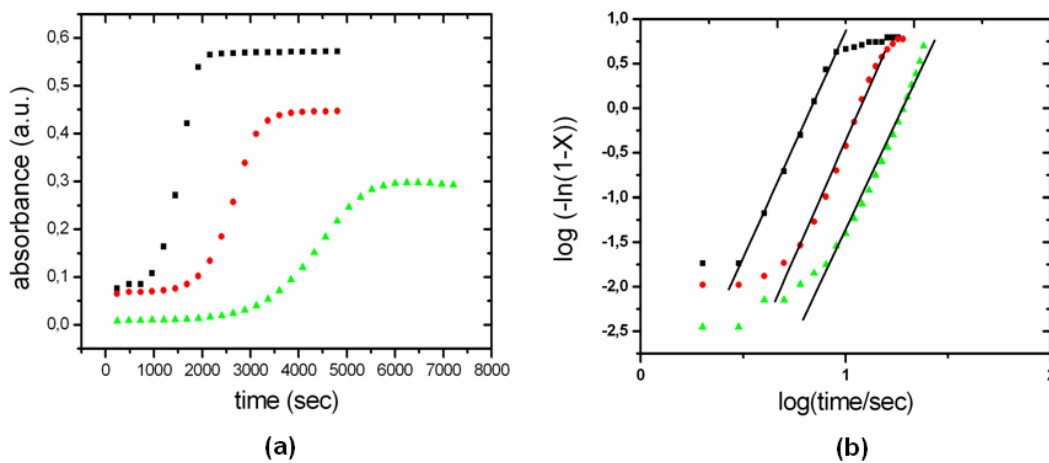


Figure 3.12 Turbidity curves showing aggregate formation of 5 mg/ml PBLG/toluene solutions which were cooled down from 70°C to 23°C (●) and 26°C (■). Data were collected at 600 nm.



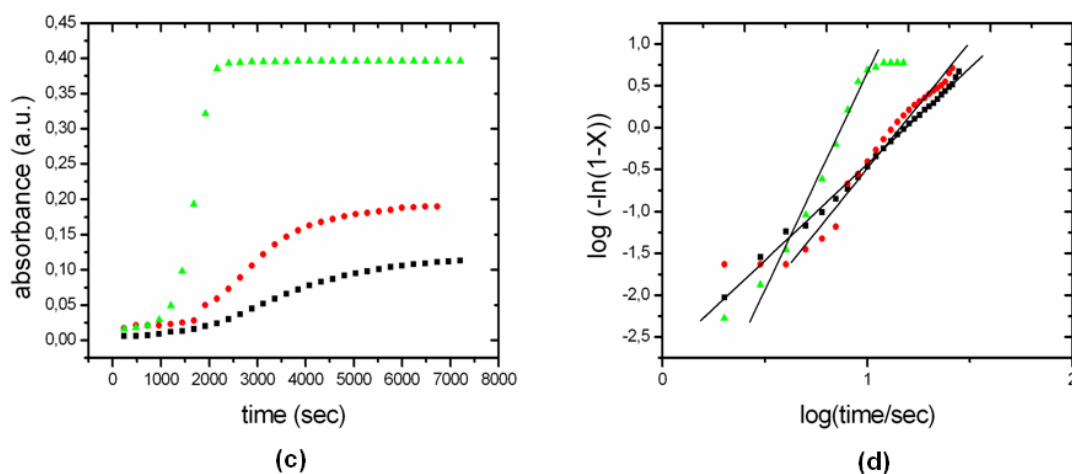


Figure 3.13 Gelation kinetics of 5 mg/ml PBLG/toluene solutions at 23°C (■), 24°C (●), 25°C (▲) (a) and fit of Avrami equation (b), Gelation kinetics of PBLG/toluene solutions with concentration of 0.4 mg/ml (■), 1.0 mg/ml (●), 3.0 mg/ml (▲) at 23°C (c) and fit of Avrami equation (d).

The gelation of PBLG/toluene solutions are extremely sensitive to temperature as shown in Figure 3.13 (a). For 5 mg/mL PGBL/toluene solution, the gelation rate and the UV-Vis scattered intensity increase as temperatures decreases from 25°C to 23°C. At all temperatures, gelation process follows sigmoidal growth which indicate nucleation and growth mechanism. To evaluate the gelation kinetics based on nucleation and growth process, Avrami equation shown below was used;

$$1 - X t = \exp(-kt^n)$$

where X corresponds to gel fraction at time (t), k corresponds to rate constant and n corresponds to Avrami exponent.

To determine the exponents, $\log(-\ln(1-X))$ was plotted as a function of \log time as shown in Figure 3.13 (b). The exponents n were calculated from the slope of linear fits and are listed in Table 3-1.

Table 3-1 The avrami exponents (n) as function of temperature (T) for 5 mg/ml PBLG/toluene solutions.

T (°C)	n
23	5.1
24	5.2
25	4.9

Table 3-2 The avrami exponents (n) as function of concentration (C) at 23°C

C (mg/ml)	n
0.4	2.3
1.0	3.0
3.0	5.2
5.0	5.1

For all temperatures, Avrami exponent was found to be 5.0 ± 0.1 . Note that 5 mg/ml PBLG/toluene solutions form a macroscopic gel at all these temperatures. An exponent of 5 suggests a heterogeneous crystallization that forms a three dimensional cone-like spherulite growth [59]. The spherulites are formed from self-assembled fibers and develops via unidirectional growth with low angle branching, similar to crystallization of some polymers [60].

A change of growth mechanism can also be found as a function of concentration at constant temperature. Figure 3.13 (c) shows UV-Vis data for different concentrations at 23°C. As concentration increases from 0.4 mg/ml to 3.0 mg/ml, the gelation rate and the scattered intensity increase. The exponents found according to Avrami analysis show significant concentration dependence (Table 3-2) varying between 2 and 5. An exponent of 2.3 for 0.4 mg/ml PBLG/toluene solution indicates the fibrillar growth controlled by homogeneous nucleation which was suggested by Tadmor et al. for

PBLG/benzyl alcohol system recently [42]. For 1.0 mg/ml PBLG/toluene solutions, exponent was found to be 3 which corresponds to a disc like growth (homogeneous crystallization) or spherulite growth (heterogeneous crystallization). The gelation kinetics of 3 mg/ml PBLG/toluene solutions is same with 5 mg/ml PBLG/toluene solutions since their Avrami exponents are both 5. An exponent of 5 together with significant increase in UV-Vis intensity for 3.0 mg/ml solution at 23°C show that the resulting structure is close to being a single 3D network as in 5 mg/ml solution.

In summary, the kinetics of molecular aggregation changes due to concentration of PBLG/toluene solutions. At concentrations below C^* , one dimensional growth and disc like growth happens. Aggregates are formed but they are not connected. At concentrations towards C^* macroscopic gel formation occurs due to three dimensional spherulite growth. Based on these results, for solution concentrations above C^* , we suggest that the gelation starts by one dimensional growth at the early stages and fibrils are formed. Then the gelation proceeds with the growth of fibers to form spherulites.

3.2.6 FT-IR measurements

It has been known that attractive interactions between polymer molecules are the major driving forces for aggregation process. In a sense, sol-gel transition depends strongly on the strength of the attractive interactions. In our case, the factor which affects the strength of intermolecular forces is the temperature. As temperature decreases, PBLG molecules arranged in an ordered fashion and form aggregates. Therefore nature of gelation on molecular level can be followed by variation of vibrational frequencies which is due to conformation change. Previously, Prystupa and Donald studied aggregation of PBLG-benzyl alcohol (BA) solutions by IR spectroscopy [61]. They followed gelation kinetics from shifts in the frequencies of amide I and ester bands. These researchers proposed that amide I band shifts to low frequencies with diminishing temperature to aggregation.

Previous literature suggests that π - π stacking interactions between PBLG helices contribute to the stabilization of structure resulting with infinite network. In this respect, stacking interactions and the resulting structure formation that leads to gelation are expected to affect the vibrational modes of the side chain benzene rings. To examine whether stacking interaction is a key factor for the gelation, we investigate the spectroscopic changes depending on state of PBLG.

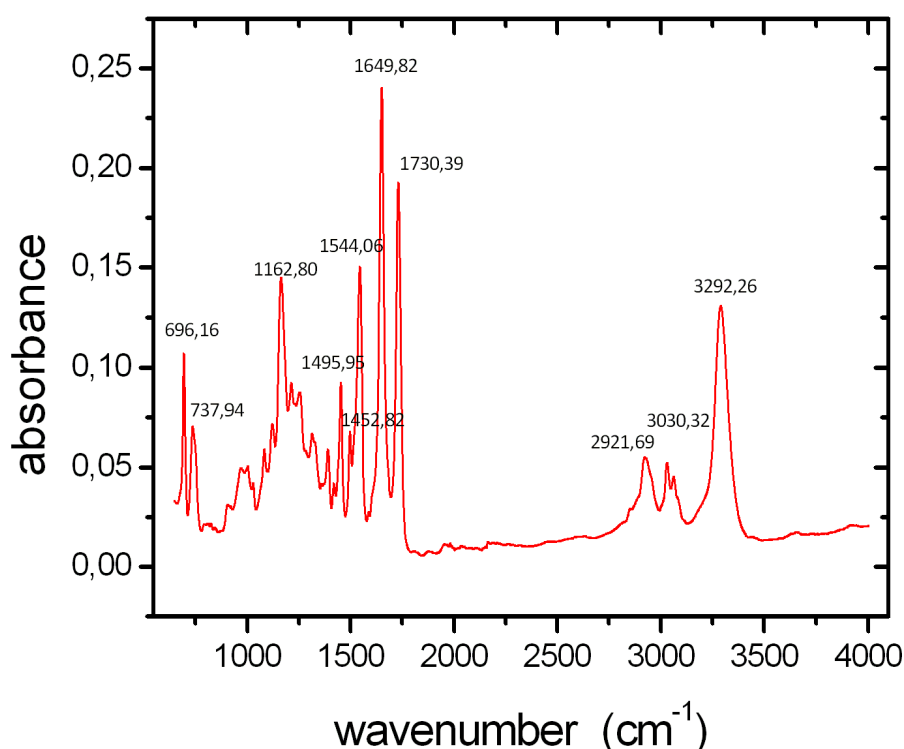


Figure 3.14 FTIR spectrum of dried PBLG/toluene gel prepared from 5 mg/ml solution by solvent casting. Measurement was taken at room temperature.

Figure 3.14 shows the infrared absorption spectrum of a dried PBLG gel. The gel was formed by drop casting technique and drying process was done by evaporating toluene at room temperature.

Table 3-3 Comparison of Vibrational Frequencies for Structured PBLG and Bulk PBLG (Literature)

Molecular Vibration	Wavenumber in cm^{-1}	Wavenumber in cm^{-1} (Literature)
N-H stretching	3292,26	3285 [62]
C-H stretching (aromatic)	3030,32	3032
C-H stretching (alkyl)	2921,69	2925
ester C=O	1730,39	1736 [34, 63]
amide I	1649,82	1655 [34]
amide II	1544,06	1550 [34]
phenyl A_1	1495,95	1495 [63]
phenyl B_1	1452,82	1450 [63]
ester C-O stretching	1162,80	1167 [63]
phenyl B_2	737,94	ca.700 [63]
amide V	696,16	614 [63]

Vibrational frequencies of dried PBLG gel and, for comparison, bulk PBLG are summarized in Table 3-3. Most characteristic bands of dried PBLG gel coincide essentially in position with literature values except for the amide V band. It seems that amide V band of structured PBLG shifts to $696,16 \text{ cm}^{-1}$. Previous researches in the literature suggest that amide bands are strongly affected by change in molecular conformation [61, 63]. In addition, amide I and amide II bands at $1649,82$ and $1544,06 \text{ cm}^{-1}$ associated with the α helical conformation of PBLG .

3.2.7 Optical Microscopy Investigations

Crystalline structures can clearly be observed by an optical microscope under crossed polarizers. Figure 3.15 (a) shows the optical micrograph of a PBLG film spin coated from 5 mg/ml PBLG-toluene solution. PBLG aggregates are seen as having darker contrast under normal illumination. It should be noted that it is not possible to compare

these aggregates one to one with the aggregates in solution. These aggregates are formed on the substrate as the toluene evaporates slowly at room temperature. However, PBLG structures that form at the early stages are expected to be preserved during spin coating. Under crossed polarizers, the optical microscopic image shows strong birefringence of the PBLG aggregates indicating ordered arrangement of PBLG helices [12, 63]. Figure 3.15 (b) and Figure 3.15(c) show the optical microscopy images under normal illumination and under crossed-polarizers, respectively, for PBLG films formed by drop casting from 30 mg/ml PBLG-toluene solution. A larger PBLG concentration was chosen in order to enhance the contrast under crossed-polarizers for crystalline regions. The sample was spread on glass wafer and bulk region occurred on the wafer due to spontaneous gelation. A bright contrast is clearly seen in Figure 3.15(c) under crossed-polarizers. This indicates the ordered arrangement of the PBLG molecules. The existence of cholesteric liquid crystalline structure of well-aged PBLG-toluene gel were previously reported for PBLG [12].

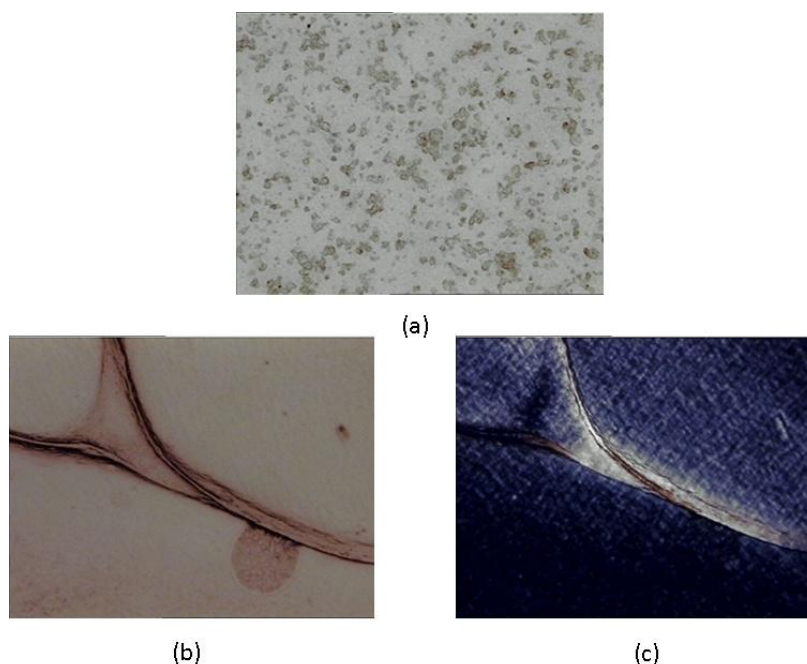


Figure 3.15 Optical microscopy images of PBLG toluene solutions; aggregated PBLG formed by spin coating at room temperature(a), 30 mg/ml PBLG-toluene gel obtained by drop casting on a glass slide at room temperature (b) and its crystalline structure under polarized light (c).

3.2.8 Morphological Investigations of PBLG Gels by AFM

To observe the morphology of dried PBLG gels, AFM measurements were carried out at room temperature for samples prepared from 0.4 mg/ml PBLG-toluene solution by spin coating at room temperature. For AFM measurements, ~200 μl of 0.4 mg/ml PBLG-toluene solution at 70°C was dropped onto a silicon wafer and allowed to cool at room temperature for 15 min on the spin coater head. The sample was then spun at 2000 rpm for 1 min to remove the remaining solution. Figure 3.16 shows the AFM height and phase images of the films.

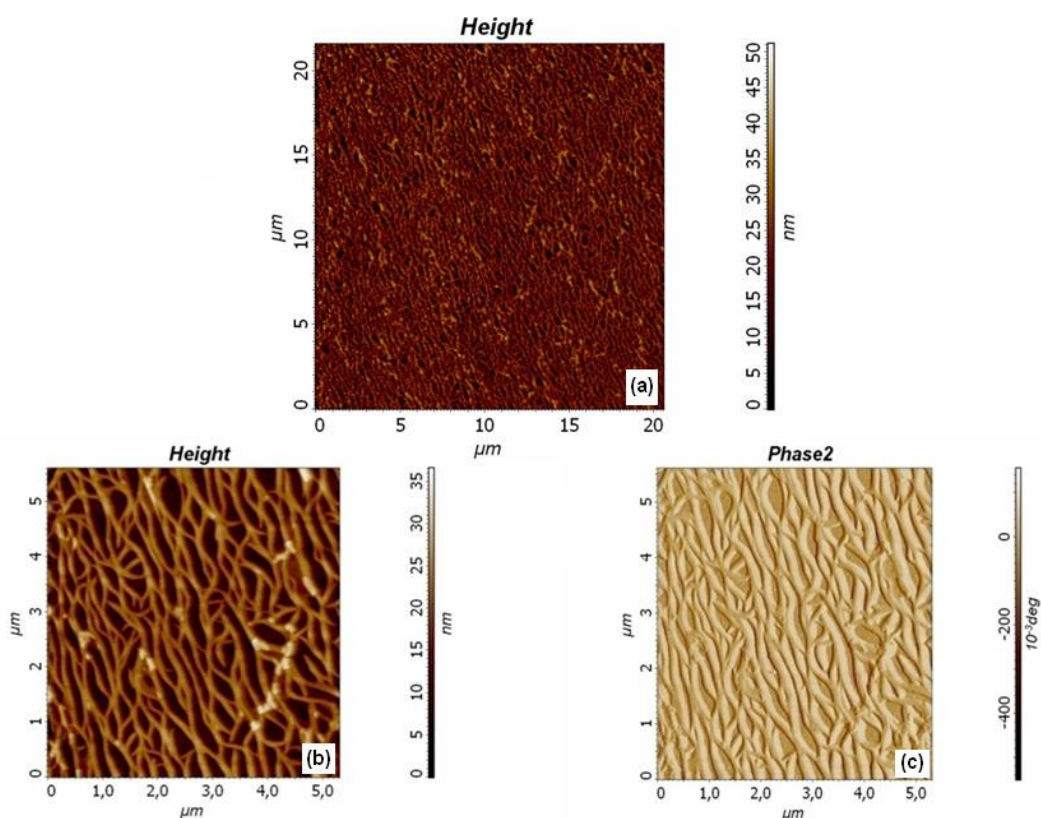


Figure 3.16 AFM micrographs of spin coated PBLG/toluene gel with concentration of 0.4 mg/ml shown as 20 μm scan (height) (a), 5 μm scan (height) (b) and 5 μm scan (phase) (c), respectively.

Figure 3.16 (a) shows the 20 μm scan height image of the PBLG film. A mesh-like network formed by branching of the PBLG fibers is clearly seen. The diameter of the fibers ranged from 100 to 200 nm and height varies between 15-18 nm. The spacing between the fibers was on the average 300 nm. It should be noted that fundamental fiber has $\sim 20\text{\AA}$ diameter [31]. Fiber thickness and the size of the pores between the fibers were found to depend on the concentration of the solution and cooling conditions. Miller et al. proposed that fibers came together and formed bundles whose diameters vary from 100 nm to 1000 nm. In addition, the distance between the fiber bundles was reported to be on the order of 1 μm [31]. Sasaki et al. observed aggregated PBLG fibers obtained from PBLG/benzyl alcohol solution as 10 nm in diameter [44]. In our measurements, concentration of the PBLG solution was 0.4 mg/ml, close to what Sasaki et al. used which was 0.5 mg/ml. In our study, well-developed bundles were obtained which may be due to different cooling conditions. Lower concentrations are expected to result in smaller diameter and larger pores.

Figure 3.16 (b) and (c) show the height and the phase image, respectively, of a 5 μm scan of the same film. Though the entanglements of the fibers and the branching are seen in more detail, it is difficult to conclude on the nature of branching and how rod-like PBLG molecules structure in the fibers.

Chapter 4 PBLG-PS /Toluene Gels

4.1 Motivation

Non-flowing state of PBLG-toluene gels arise from the self assembled fibrillar network. Self assembly is governed by strong π - π interactions between benzyl side groups of PBLG, in addition to dipolar interactions. Previously, Prystupa et al. reported that aggregation process of PBLG chains has been side by side [61] in which benzyl groups are at the outer surface of PBLG helices [54]. Polymers especially those with aromatic moieties, can interact with PBLG via π - π stacking with side chain phenyl rings of PBLG. We expect that intermolecular stacking interaction between PBLG molecules and such a polymer to promote formation of a composite gel and to improve the physical properties of PBLG-toluene gels.

To examine the effect of an additive on physical properties and gelation kinetics of PBLG-toluene gels, we incorporated polystyrene (PS) into the system. The reason to choose PS is that it has phenyl side groups attached to the backbone which can interact with PBLG benzyl group via π - π stacking. In addition PS is highly soluble in toluene.

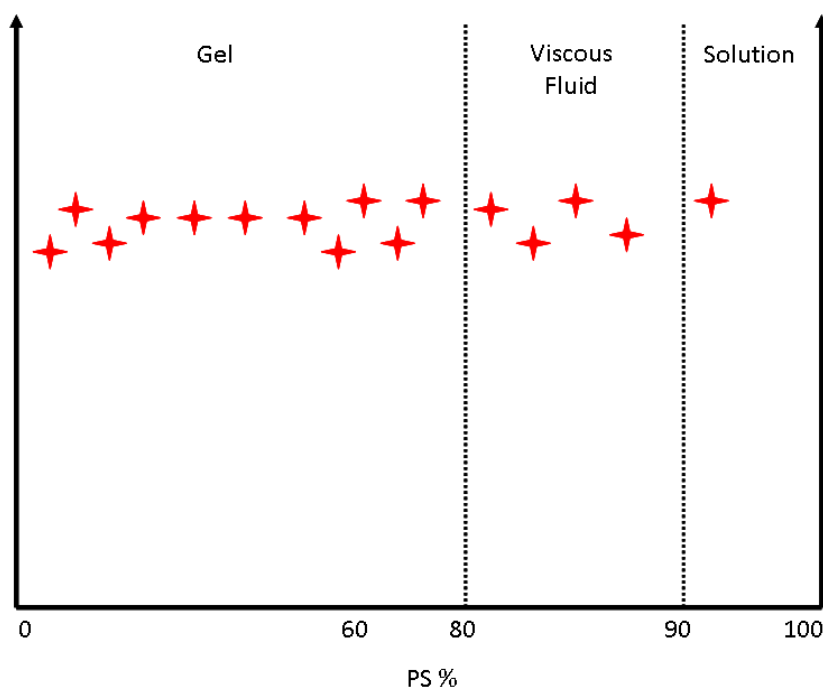
Notwithstanding a vast number of articles have been published on the investigation of gelation phenomenon of PBLG systems, there is no report in the literature that aims at studying dynamics of the PBLG organogels by incorporation of additives. There are some recent reports that deal with composite gel systems [10] that is not relevant to PBLG organogels. It is noteworthy to mention that this is the first study of a PBLG / additive composite system. It is therefore expected to succeed in forming composite gels without disrupting the interactions between PBLG chains. In the present study, for the first time, additive effect on assembly of PBLG molecules is investigated. For aggregate formation and structure analyses, we used similar characterization techniques

as in Chp. 3, namely DLS, UV-Vis Spectroscopy, Micro-Viscometer, optical microscopy and AFM.

4.2 Results & Discussion

4.2.1 Effect of PS concentration on Gelation

To study the effect of polystyrene (PS) on the gelation of PBLG-toluene system, PS having molecular weight of 2000 g/mol was added into the PBLG/toluene solutions. The mixed solutions containing different amounts of PS were homogenized at 70°C for 2 h. Visual observations were recorded after solutions were kept at 23°C for 2h.



Scheme 4.1 Diagram showing the state of PBLG-PS/toluene solution depending on loading percentage of PS. The homogenized solutions were kept at 23°C for 2 h and then subjected to gravity. The experimental data shown as ★

Scheme 4.1 illustrates the state of PBLG/PS-toluene solutions with increase in weight percentage of PS. Varying weight percent loads of PS were incorporated into 5 mg/ml PBLG-toluene solution for comparison. Visual observations were recorded after

subjecting samples to gravity for 2 hour. We observed that the incorporation of low percentage of PS did not destroy the stability of PBLG-toluene gel. To determine the critical loading concentration in weight percentage of PS for the gelation above which the solution exists as a viscous fluid, PS amount was increased above 60%. Interestingly, even with addition of 82% PS, non-flowing PBLG gel was obtained based on our visual observations. Further incorporation of PS weakened the gel network and caused gel to flow down when the vial was turned upside down. Once the weight percentage of PS reached to 92%, instead of a viscous fluid, only clusters were formed and a solution was obtained.

PS was successfully introduced into the PBLG-toluene system due to being highly soluble in toluene. The resulting organogel retained its physical state as solid-like until the loading percentage of PS reached to 82%. A very high loading PS into the PBLG gel without breaking down network may indicate that PS molecules interact both with PBLG molecules through π - π stacking interactions arising from aromatic moieties and with toluene; and hence stabilize the macroscopic structure. At high loading percentage which is above 92%, no gel formation was observed in PS/PBLG-toluene system which is attributed to perturbation of gel organization with the addition of PS molecules. We interpret that loading above of 92% PS into the system blocked the interactions of PBLG chains with each other and prevented structuring.

4.2.2 Determination of PS effect on gelation by DSC Measurement

The thermoreversible behavior of the PS-PBLG/toluene gel has been investigated by means of DSC to figure out effect of PS on the gel. Composite organogel was prepared from 10 mg/ml PBLG-toluene solution containing 60% PS by cooling hot solution to 23°C. The gel was then put in DSC to observe the melting peak. A scan rate of 5°C/min was used. It should be noted that heating and cooling curves were obtained by following the same protocol as for PBLG-toluene system (Figure 3.3)

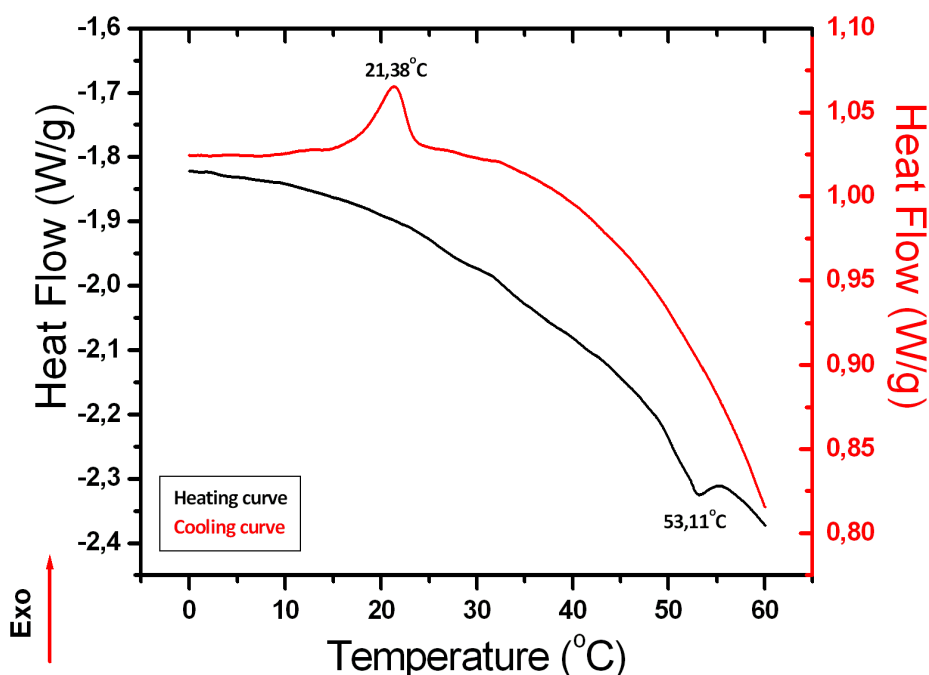


Figure 4.1 Heating and cooling DSC cycles of 10 mg/ml PBLG-toluene composite gel including 60% PS. Exothermic peak at 21.38°C corresponds to gelation and endothermic peak at 53.11°C corresponds to melting transition. Scan rate was 5°C/min.

Figure 4.1 shows the phase transition temperatures of composite organogel of PBLG. The transition from gel to solution results in an endothermic peak which was observed at 53.11 °C. In addition, the exothermic peak at 21.38 °C corresponds to solution to gel transition.

To figure out the effect of incorporating PS in the PBLG gel matrix, we used composite gel having a high loading percentage of PS (60%). As incorporated amount of PS increases, PS is expected to dominate the gel network and affect the physical properties of PBLG-toluene gels. Based on DSC results, the incorporation of PS does not influence the thermoreversibility of PBLG-toluene organogel. However, transition temperatures shift towards to higher temperatures with addition of PS into the gel matrix. T_{gel} of composite sample is 1.65°C higher than T_{gel} of native one and the

organogel alone shows a T_{melting} at 50.72°C (See Figure 3.3) while the composite with 60% PS shows at T_{melting} at 53.11°C (See Figure 4.1). This may indicate that the presence of PS facilitates aggregate formation rather than perturbing fibrillar structure. One of the possible reason is that dissolved PS molecules interact with the PBLG helices via π - π stacking of aromatic groups hence enhances aggregate formation [64]. Another argument with the aim of explaining PS influence on gel formation is that PS molecules can serve as nucleation center for gelator molecules, i.e. PBLG helices, during self-assembly so it speeds up the gel formation regarding to PBLG organogel [65]. The melting temperature being higher with PS compared to the native gel also indicates a more stable gel network. Although we did not have any direct evidence about the role of PS in gel formation, the fact that gel is formed up to 82 % PS by weight together with higher melting and gelling temperatures in DSC can be interpreted as the favorable contribution of PS to gelatin kinetics and gel stability.

4.2.3 Investigation of PS effect on gelation kinetics by DLS

The literature includes studies which are based on following gelator-additive interaction via Dynamic Light Scattering (DLS) [66]. In our study, we have also used DLS for comparing aggregation of PS-PBLG/toluene solutions with PBLG/toluene solutions. To examine the structure formation during gelation of PS-PBGL/toluene solutions, the time dependence of aggregate size at different loading percentages of PS and temperatures was monitored via DLS.

Since DLS measurements depend on the diffusion of the aggregates in the solution, we have chosen the measurement temperature as 26°C which is at the upper end of the gelation temperature. 5 mg/ml PBLG/toluene samples containing 0.4, 0.6, 0.8 and 1.0 % PS were used for the measurements at 26°C. At 26°C for higher incorporation percentage of PS at 5 mg/ml PBLG/toluene, DLS measurements also suffered from too fast growth of aggregates. Therefore, to observe gelation kinetics of PS dominated solutions at 26°C, 3 mg/ml PBLG/toluene solution containing 60% PS was chosen. To

observe the effect of temperature on the structure formation during gelation of PS-PBLG/toluene solutions mentioned above, DLS data were taken also at 30.0°C.

PS-PBLG/toluene solutions were homogenized at 70°C in oven and then placed into the Dynamic Light Scattering instrument where the sample cell temperature was set constant at 26°C and 30°C, respectively. 500 measurements were carried out, each at 10 second run time. Hydrodynamic diameters of aggregates were obtained from intensity correlations using toluene viscosity as the medium viscosity.

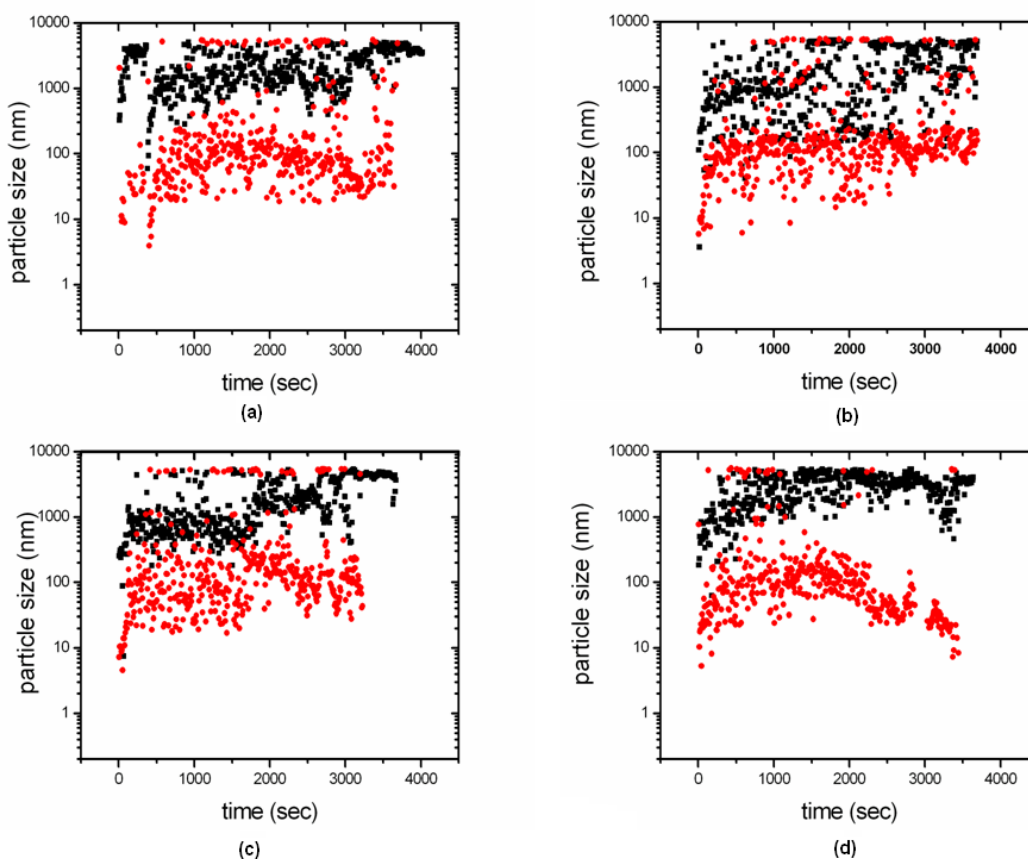


Figure 4.2 Aggregate size growth as a function of time measured for homogeneous 5 mg/ml PBLG-toluene solutions containing (a) 0.4%, (b) 0.6%, (c) 0.8% and (d) 1.0% PS recorded at 26°C. The size of first peak is represented by (■) and second peak is represented by (●)

Figure 4.2 shows aggregation process of PBLG/PS solutions containing different percentages of PS at 26°C. Aggregate growth of PS-PBLG solutions differs due to percentage of PS incorporation. With addition of PS to PBLG solutions, aggregate size shows very broad distributions over time. For PBLG solutions containing 0.4% PS, two aggregate sizes were observed. Since DLS data was scattered, it is difficult to determine the time at which aggregate size reaches the maximum. With a further increase in PS addition, more scattered data was obtained. Although size distributions interfere with each other, the growth rate of aggregates can be clearly observed. The aggregate size reaches to 1000 nm in ~300 seconds (see Figure 4.2 (b)). Figure 4.2 (c) shows that growth rate of aggregates increases with incorporation of PS. In ~200 seconds, size of PBLG aggregates increases towards to 1000 nm. The last data given in Figure 4.2 (d) corresponding to 1% PS exhibits more steady growth in comparison with other samples. Two different sizes were observed as the fluctuations reduced. Growth rate of the aggregates was relatively faster; in ~150 seconds 1000 nm aggregates were obtained and in ~300 seconds aggregate size reached a maximum of ~5000 nm.

We studied with PS-PBLG solutions with low percentage of PS to determine effect of additive before the system was saturated with PS. PS-PBLG/toluene solutions show two different intensities indicating that there are two types of aggregates in the solution. Also sizes are highly scattered. This could be explained by monitoring free PS molecules floating randomly and structuring PBLG-PS molecules at the same time. Large size indicates the gel formation which is additive independent, second is the PS-toluene solution. As a result, we obtained highly complicated aggregation process due to interference of PS molecules and aggregates of PBLG-PS. The instability of particle size might be associated with the interaction between PS and PBLG molecules.

It is expected that PS molecules participate in formation of PBLG aggregates probably due to π - π staking interactions. However, the results obtained by addition of PS in PBLG solutions were found to be similar with results of PBLG/toluene solutions

indicating that PS had no important effect on gelation onset. We interpreted that PS may affect the later stages of gelation which cannot detect by DLS. The addition of PS into PBLG fibers may contribute to better branching of PBLG fibers which will result in faster growth of a 3D network. This 3D PBLG network can further be stabilized by the PS molecules acting as a bridge between PBLG benzyl groups and the toluene molecules.

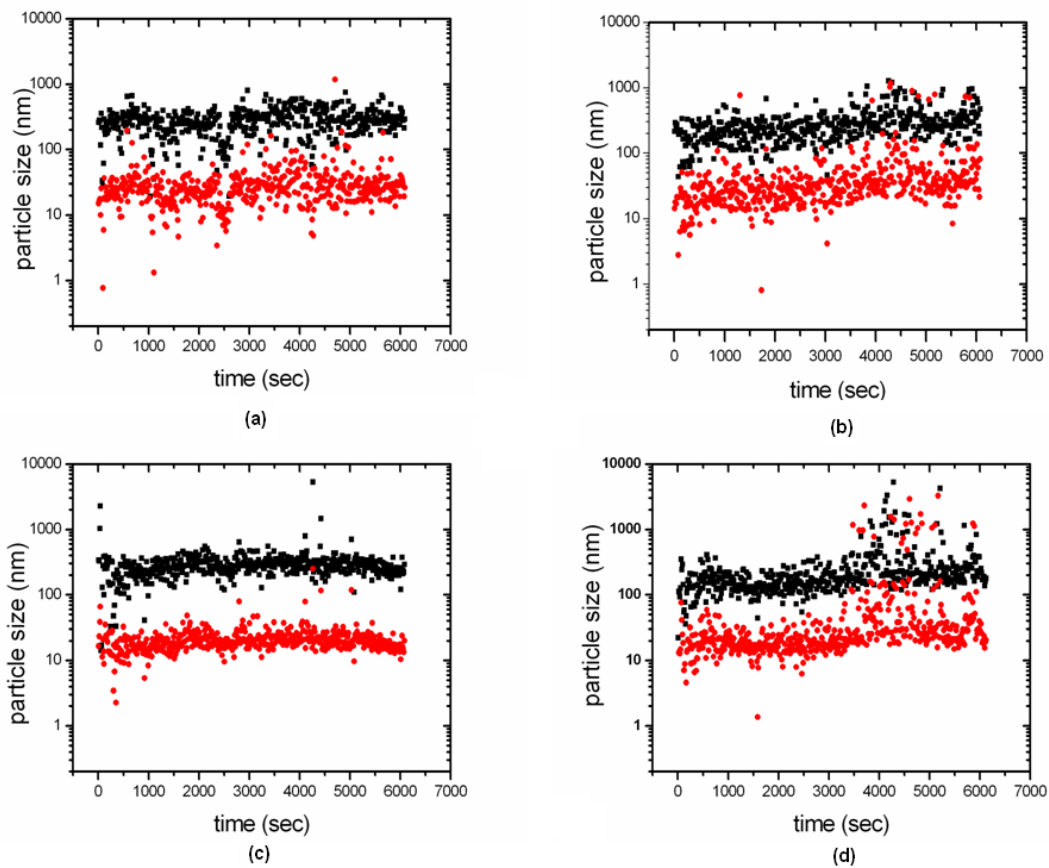


Figure 4.3 Aggregate size growth as a function of time measured for homogeneous 5 mg/ml PBLG-toluene solutions containing (a) 0.4%, (b) 0.6%, (c) 0.8% and (d) 1.0% PS recorded at 30°C. The size of first peak is represented by (■) and second peak is represented by (●)

Further investigations of PS effect on gelation were done at 30°C to compare growth rates and aggregate sizes at slower gelation. However we could not observe any dramatic difference between PBLG gel (Figure 3.6) and PBLG-PS gels (Figure 4.3). For all solutions shown in Figure 4.3 two different aggregate sizes were observed which stabilized at 30 nm and 300 nm which were observed as 10 nm and 200 nm for PBLG-toluene solution. The larger size may originate from the viscosity change of the solution by addition of PS. The similarity of DLS data for PBLG-PS/toluene and PBLG/toluene at 30°C shows that the driving force for gelation is the intermolecular interactions between PBLG molecules in both systems. Once this driving force gets dominant, PS contributes to gelation kinetics and stability by interacting with the self-assembled structures.

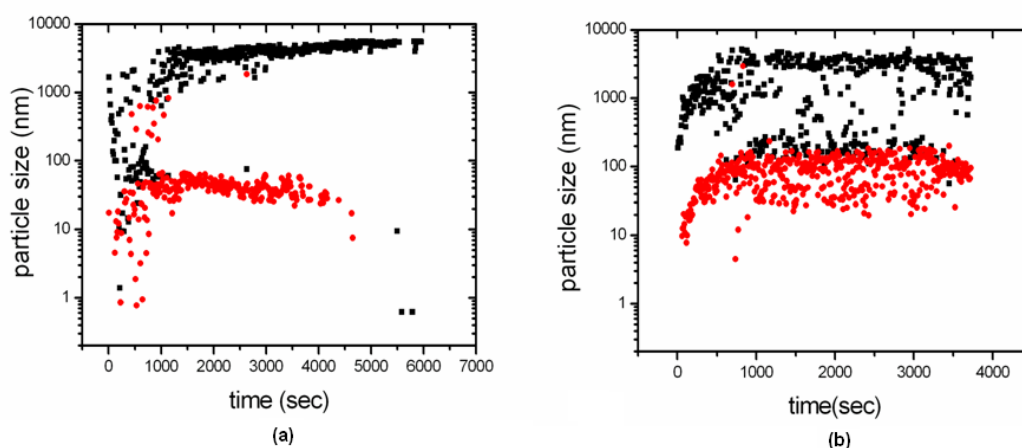


Figure 4.4 Aggregate size growth as a function of time measured for homogeneous 3 mg/ml PBLG-toluene solutions containing (a) 60% PS and (b) 0% recorded at 26°C. The size of first peak is represented by (■) and second peak is represented by (●)

To investigate gelation kinetics of PS dominated PBLG solutions, 3 mg/ml PBLG/toluene solution containing 60% PS was used for DLS measurement. Figure 4.4 shows DLS results of PS/PBLG solution and PBLG solution at the same concentration for comparison. Comparing the PS-PBLG solution with PBLG solution, one can observe that aggregate size of PS-PBLG solution is distributed relatively uniform while

aggregate size of PBLG solution looks scattered. Both aggregates in PS-PBLG solution and in PBLG solution reached a maximum of 5000 nm at similar growth rate of aggregates.

4.2.4 Viscosity Measurements of PS/PBLG organogels

Concentration effect on gelation by following change in viscosity during gel formation was discussed previously. It was found that PBLG/toluene solutions showed increase in viscosity with concentration due to growth of aggregates. To examine the effect of PS on gelation kinetics, we have measured viscosity of PS-PBLG/toluene solutions.

Similar to the choice of 26°C for PBLG/toluene solutions, the same temperature was chosen for PS-PBLG/toluene solutions to be able to observe gelation kinetics over large time intervals. Increase in viscosity was examined during gelation of 5.0 mg/ml PBLG solution including 60% PS. Growth of aggregates limits taking further measurements with time similar to lower temperatures. Homogenous PS-PBLG/toluene solution was filled into capillary and then placed in capillary holder where the temperature was kept constant at 26°C. The inclination angle of the capillary was set to 30°.

The Figure 4.5 shows comparison of kinetics of PBLG/toluene gels formation with and without PS. The viscosities of PBLG/toluene and PS-PBLG/toluene solutions increased in the same fashion at first 1500 seconds. After 1500 seconds, composite gel shows more drastic increase in viscosity relative to native one. Composite gel reaches 42 mPa.s in ~2300 seconds on the other hand it takes more time (~3500 seconds) for native gel to reach as same viscosity.

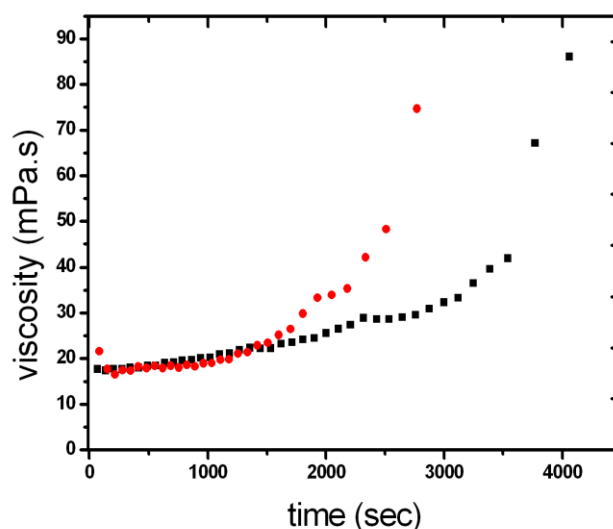


Figure 4.5 Time dependency of viscosities of 5.0 mg/ml PBLG/toluene solution (■) and 5.0 mg/ml PS-PBLG/toluene solution containing 60% PS by weight (●) at 26°C.

Previously, Wang and Chen have investigated gelation kinetics of SWCNTs incorporated hydrogel [17]. They found out that process of gel formation was accelerated when SWCNTs was added in the system. Our results obtained above are close to Wang and Chen et al.'s results that the incorporation of PS into the PBLG gel had an obvious impact on gelation process. During the first 1500 seconds of gelation, composite gel and native gel exhibit similar increase in viscosity. This result indicates that onset of gelation is not affected by PS incorporation which is consistent with DLS measurements. The intermolecular interactions between PBLG chains aggregating to form microfibrils might be independent from the presence of PS molecules. As gelation progresses, viscosity of PS-PBLG/toluene solution deviate from PBLG/toluene solution. This suggests that addition of PS in the system accelerates the branching and maybe attachment of PBLG aggregates resulting in 3D network. Based on viscosity results, we interpret that PS molecules act as branching points or crosslinking points for aggregated PBLG domains and results in faster macroscopic network construction.

4.2.5 Turbidity Measurements of PS-PBLG gels by UV-Visible Spectrometer

As mentioned earlier, UV-Visible Spectrometer can be used to follow gelation kinetics by investigating change in turbidity. To understand the effect of PS addition on gelation kinetics of PBLG/toluene gels, absorbance change of PS-PBLG/ toluene solutions was examined as a function of time by means of UV-Visible Spectrometer.

5.0 mg/ml PBLG-toluene solution containing (1%, 2%, 60% by weight) PS were chosen for the measurements. 20 spectra were taken consecutively in the wavelength range of 200-1100 nm after the homogenized hot solution was placed into the sample holder whose temperature was kept constant at 23°C. One spectrum took nearly 4 minutes. So the total time for the whole measurement was ~ 80 min. The measurement time was chosen long enough to observe the final state of gelation. To analyze kinetics of gelation more precisely, absorbance change was plotted against time at 600 nm.

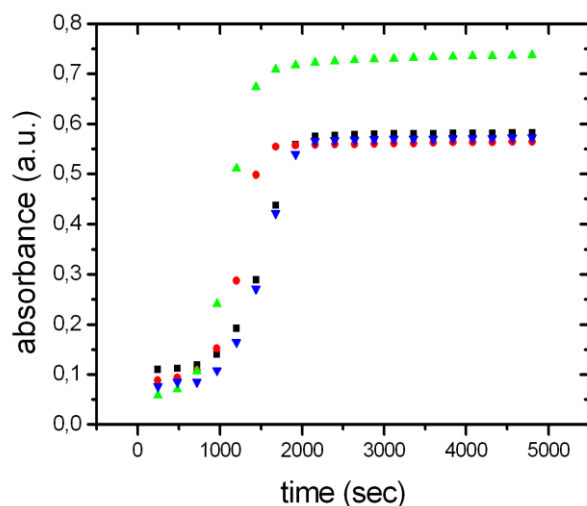


Figure 4.6 Turbidity curves showing aggregate formation of 5 mg/ml PBLG/toluene solutions containing %1 (■), 2% (●), 0%(▲)and 60% (▲) PS as a function of time. Data were collected at 600 nm since cooling from 70°C to 23°C.

Figure 4.6 demonstrates the gelation kinetics of PS/PBLG solutions as a function of time. The gelation kinetics was obtained by following the changes in absorbance over time. At 23°, gelation process of PBLG solutions with low loading percentage of PS (1% and 2%) show similar trend with PBLG solution. Maximum scattered intensity obtained from these solutions was 0.55. With a high loading percentage of PS, aggregated PBLG scatters more light resulting in higher scattered intensity which reaches to 0.7. In other words, resulting gel was thicker and denser than native one in the presence of PS.

To examine the critical gelation time and absorbance change for each concentration, sigmoidal fit was done to turbidity curves of PS/PBLG solutions shown in Figure 4.7. We expected an increase in absorbance change and decrease in critical gelation time with loading percentage of PS. As PS was incorporated into PBLG-toluene solutions, gelation time decreases. Figure 4.7 shows that 1% incorporation of PS does not affect the gelation time remarkably. According to our previous finding, critical gelation time of 5 mg/ml PBLG-toluene gel is ~1500 seconds which is close to PBLG/toluene solution containing 1%PS (~1500 seconds). This indicates that incorporated PS has no significant effect on macroscopic gelation when the percentage was lower than 1%. As loading percentage of PS into PBLG solution increase to 2%, critical gelation time dramatically reduces to ~1200 seconds. It is obvious from Figure 4.7 that gelation process accelerates more significantly in PS dominated PBLG/toluene solutions. Gelation takes place in ~1000 seconds and slows down to reach its final state which is relatively faster considering other solutions. In addition, scattered intensity increases with incorporation of PS into the system. In the presence of PS, aggregates grow larger in size therefore scattered intensity reaches to higher values.

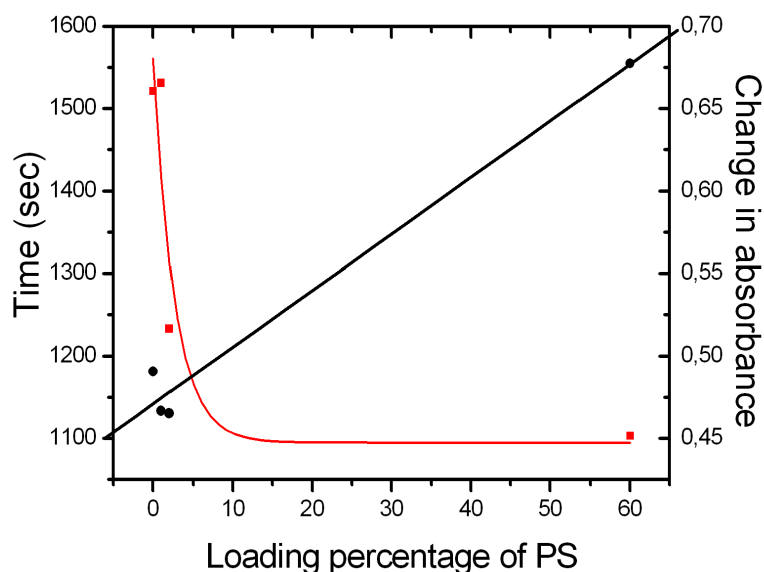


Figure 4.7 Critical time for gelation (■) and change in absorbance (●) as a function of loading percentage of PS. Determination was done by applying sigmoid fit to 5 mg/ml PBLG/toluene solutions containing 0%, 1%, 2% and 60% PS as shown Error! Reference source not found..

The results presented above indicate that incorporation of PS become effective in 3D network construction when the loading percentage is between 1-2%. Increase in absorbance change with respect to PS amount could be explained by formation of larger aggregates in the presence of PS. We interpret that PS molecules facilitate the interconnection of aggregated PBLG domains therefore macroscopic gel forms in a shorter time. The time decay as a function of PS incorporation emphasizes that there is physical interactions between PS and PBLG molecules. Otherwise gelation time would not alter significantly with addition of PS in PBLG solutions. The interaction may arise from aromatic moieties of PBLG and PS molecules which is also known as π - π stacking interactions. In detail, PS can stabilize the system via π - π interactions therefore the process of PBLG organogel was accelerated [17].

4.2.6 Optical Microscopy Investigations for PS-PBLG organogels

Crystalline structure of PBLG/PS-toluene system was investigated by illuminating dried PS-PBLG gel under polarized light by optical microscope. The purpose of this examination was monitoring the existence of an ordered structure considering the fact that percentage of PS in the system was extremely high relative to PBLG.

Gel of PS-PBLG was from 5 mg/ml PBLG/toluene solution including 80 % PS by weight. Dried gel was obtained by evaporating toluene slowly at room temperature. Dried gel was investigated under polarized light to observe crystalline domains.

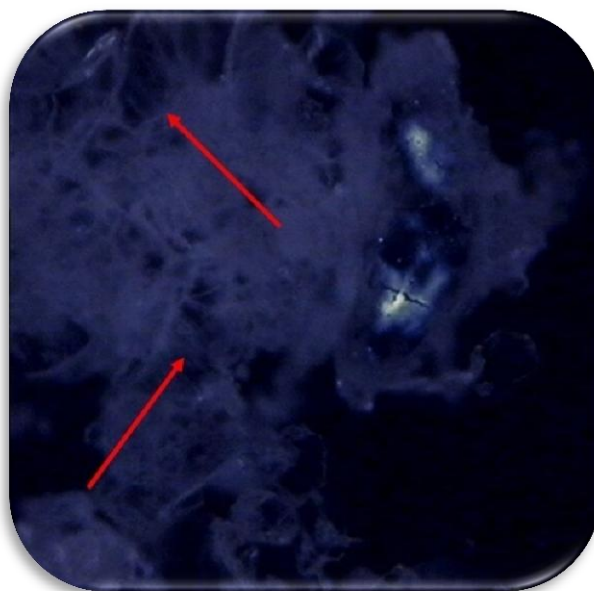


Figure 4.8 Optical micrograph of dried PS-PBLG organogel under crossed polarized light. Arrows indicated the fibrillar network of the residue

Figure 4.8 shows the optical micrograph of dried PS-PBLG gel. Existence of a contrast appearance is clearly seen due to having crystalline domains. This crystalline structure belongs to structured PBLG molecules since atactic PS is a non-crystalline polymer. This indicates that PBLG can form fibrillar network within PS matrix. The high loading percentage of PS does not block gelation of PBLG. Also, arrows shown in Figure 4.8 indicate fibrillar network of PBLG in PS matrix.

4.2.7 Morphological Investigations of PS-PBLG Gels by AFM

To determine the morphology of PS-PBLG organogels and the dispersion of PS, AFM measurements were carried out at room temperature for samples prepared from 0.4 mg/ml PBLG-toluene solution containing 60% PS by spin coating at room temperature. For AFM measurements, ~200 μl of 0.4 mg/ml PS-PBLG/toluene solution at 70°C was dropped onto a silicon wafer and allowed to cool at room temperature for 15 min on the spin coater head. The sample was then spinned at 2000 rpm for 1 min to remove the remaining solution. Figure 4.9 shows the AFM height and phase images of the film.

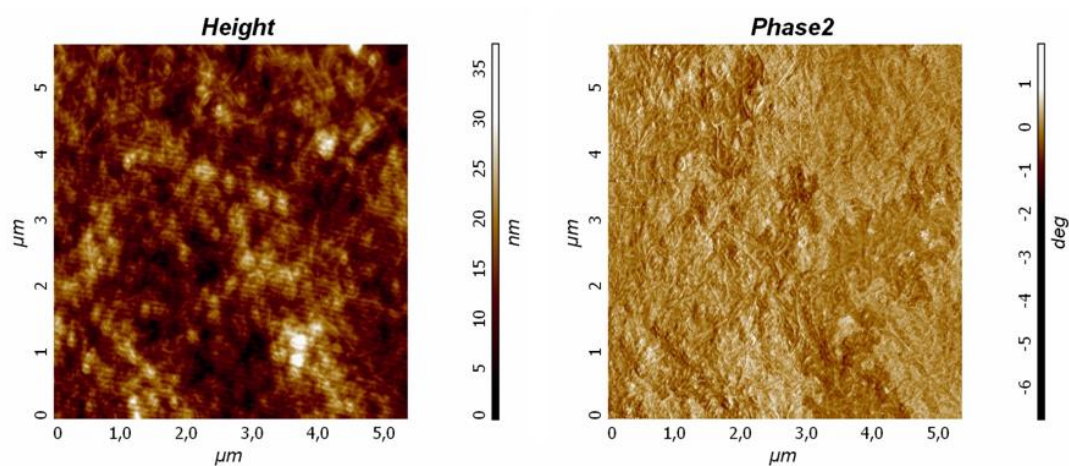


Figure 4.9 AFM height (a) and phase (b) images of spin coated PBLG gel from 0.4 mg/ml PBLG/toluene solution including 60%PS.

Figure 4.9 shows the AFM height and phase images of dried PBLG gel containing 60% PS. It is clearly seen that a mesh-like network exists. Fibers are obvious especially in the phase images of the sample. It should be noted that AFM images of PBLG dried gel (see Figure 3.16) and PS-PBLG dried gel (see Figure 4.9) look quite different. As mentioned, PBLG gel had a branching neat network which involves empty spaces between the fibers. On the other hand composite gel seems more complicated, fibers cannot be recognized easily contrary to the native one. The empty space between PBLG fibers was on the average of 300 nm. However we could not observe such empty spaces

between fibers in PBLG/PS gel. This indicates that PS acts as a matrix in the system, therefore nanospaces are filled with PS.

Chapter 5 Conclusions

Homogeneous PBLG/toluene solution evolves towards the formation of gel in dilute concentration regime when it was cooled. In the first part of the thesis, we studied the gelation kinetics of PBLG/toluene solutions as a function of time, temperature and concentration. It was found that the critical gelation temperature (T_{gel}) for 5.0 mg/ml PBLG/toluene solution was between 23-26 °C based on visual observations. A more accurate determination of gelation and melting transitions of PBLG/toluene gels were done by DSC. The measured gel melting and gelation temperatures were 51.04°C and 19.65°C, respectively. The critical concentration (C^*) which formed a macroscopic gel at 23°C was determined between 3-5 mg/ml by vial inversion. Various concentrations of PBLG toluene solutions close to C^* were used for DLS, viscosity and UV-visible spectrometer measurements to examine concentration dependence of gelation as a function of time. Aggregate formation in PBLG/toluene solutions with different concentrations at 26°C (T_{gel}) was followed by DLS as a function of time. Two aggregate sizes were observed at 26°C. Based on DLS results, aggregate size and growth rate of aggregates were found to increase with increasing PBLG/toluene concentration. In addition, aggregate growth with concentration resulted in increase of viscosity at 26°C. The ultimate viscosity of solutions was remarkably different from each other. Turbidity measurements taken at 600 nm via UV-visible spectrometer confirmed that dilute solutions scattered less light than concentrated solutions depending on aggregate size. Gelation time determined from turbidity curves of PBLG/toluene solutions shifted towards shorter times with increasing concentration. Since PBLG solutions were too sensitive to temperature, DLS was also used to investigate temperature effect on gelation of 5 mg/ml PBLG/toluene solutions. As the temperature reduced from 30 to 26°C, aggregates grew in size and reached to several micrometers. Temperature dependence of gelation was also observed in turbidity curves of PBLG/toluene solutions taken at various temperatures. At 26°C, solution did not

show any change in absorbance over time while it showed a drastic increase in absorbance at 23°C. Though growth of aggregates was monitored via DLS at 26°C, UV-visible spectrometer did not detect any absorbance change at that temperature. Avrami equation was used to determine the nature of the structure growth process in PBLG/toluene solutions. The Avrami exponent n was found to be between 2-5 depending on the PBLG/toluene concentration. The crystalline structure of PBLG network was detected under crossed polarized light via optical microscope. AFM measurements revealed the fibrillar network of PBLG which assembled to form aggregates.

In the second part of the thesis, composite organogel was prepared by incorporating PS into PBLG/toluene solutions. It was found that PS loading above 92% by weight broke down the macroscopic gel. Kinetic studies on PS-PBLG/toluene organogels were carried out by incorporating low percentage (0.4-1% by weight) and high percentage (60% by weight) of PS into PBLG/toluene solutions. Melting endotherm and gelation exotherm were observed at 21.38° and 53.11°C, respectively. From DLS, broad size distribution was obtained for PBLG/toluene solutions including low percentage of PS. As amount of PS loading increases, aggregates grew in size in shorter times and distributed more uniformly. With a higher loading percentage of PS (60% by weight), scattering of aggregate size minimized and two sizes of aggregates were obtained. In PS-PBLG/toluene solutions and PBLG/toluene solutions, size evolution of aggregates was similar. Viscosity data showed that the presence of PS accelerated gelation of PBLG/toluene solutions. Turbidity measurements also supported that critical gelation time decreased with increasing PS incorporation. In addition, scattered intensity increased significantly when PS became dominant in the solution. The fibrillar network formation of PS-PBLG/toluene gels was confirmed by optical microscope. Under crossed polarizer, PS-PBLG dried gel showed strong birefringence indicating crystalline structure. Fibrillar aggregation of PBLG formed in PS matrix was clearly observed by AFM.

Based on these experimental findings, we propose a model for the gelation kinetics of PBLG in toluene. The model assumes that different analysis techniques capture different stages of the gelation mechanism. Being sensitive to very small aggregate sizes of the order of nm, DLS data provides information about the early stages of the gelation in which individual α -helical PBLG molecules combine to form the nuclei of the self-assembled structures. Viscosity measurements are sensitive to the intermediate stage of the gelation where the growing aggregates act independently but contribute to the viscosity. Turbidity data provides information about the last stage of gelation where the aggregates come together to form a macroscopic gel.

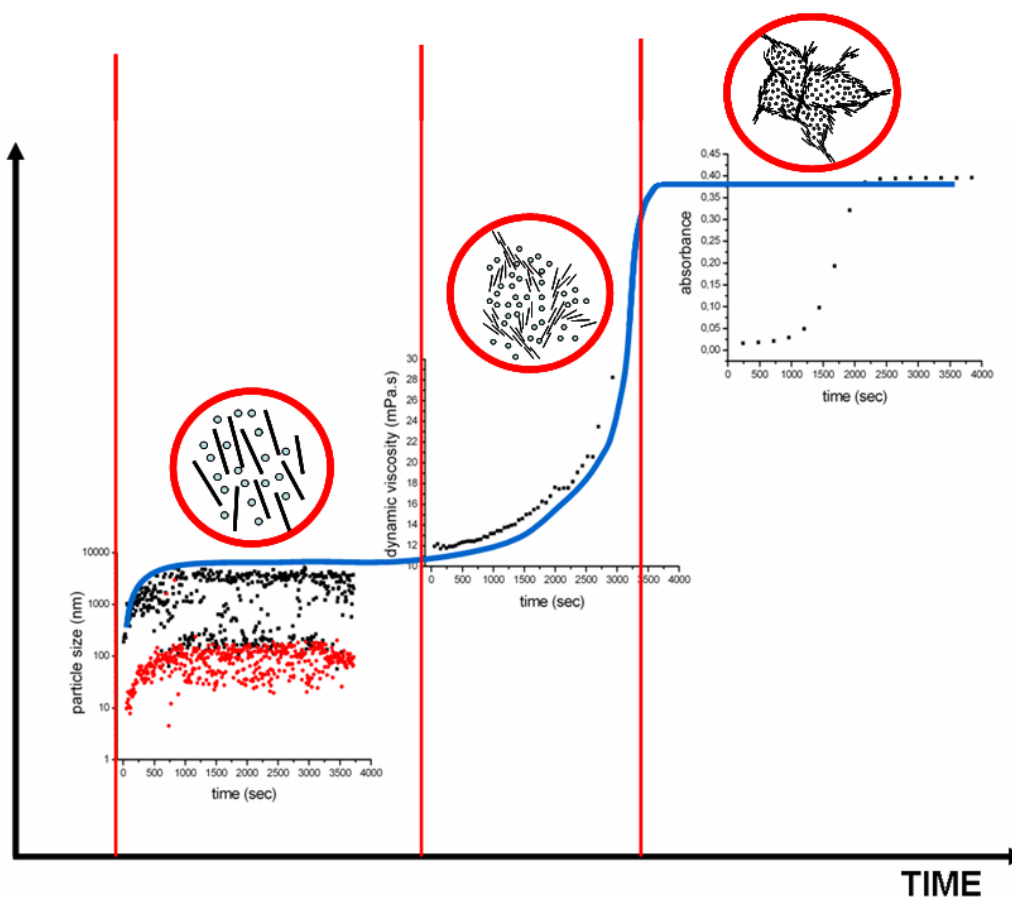


Figure 5.1 Model proposed for gelation of PBLG in toluene

Figure 5.1 schematically shows the three stages in the gelation of PBLG in toluene together with the representative data: (i) Structure formation: Rod-like α -helical PBLG molecules are dissolved homogeneously at high temperatures ($\sim 70^\circ\text{C}$). At room temperature the interactions of PBLG molecules (dipolar interactions and π - π stacking) dominate and PBLG molecules nucleate to form self-assembled fibers. These fibers grow anisotropically with significant branching and thus can be considered as spherical aggregates. The size of these aggregates reach a steady state value according to DLS measurements. (ii) Aggregate growth: The growth of PBLG aggregates consisting of self-assembled fibers continue in time. This later growth can be out of the range of DLS sensitivity, but was captured by viscosity measurements. As the micrometer sized aggregates grow in time, the viscosity increases. (iii) Aggregate fusion: The growing aggregates touch each other and interact which results in fusion of smaller aggregates into a larger one. This is the stage in which the macroscopic gel forms by fusion of all aggregates into one single macroscopic aggregate consisting of 3D network of fibers. As the aggregates fuse together, turbidity of the sample increases. This stage were captured by scattering of UV-Vis light. For 5 mg/ml PBLG/toluene solutions at 30°C the macroscopic gel did not form and the scattered light intensity did not change with time. But at 26°C , a large increase in the intensity of the scattered light was observed confirming the sensitivity of the turbidity measurements to macroscopic gelation.

The fusion of aggregates is remarkably temperature and concentration dependent. Time evolution of fusion (macroscopic gelation) was analyzed on the basis of Avrami equation. At the early stages of gelation one dimensional growth results in formation of fibrils, proceeds with branching and growth of these fibrils into aggregates and macroscopic gelation only occurs if these aggregates develop into spherulites and fuse into one.

With increasing concentration, aggregation process accelerates possibly by intermolecular interactions between PBLG helices. Above T_{gel} , thermal energy

dominates over intermolecular interactions which drive PBLG aggregation. At dilute concentrations, aggregates do not grow further since the large intermolecular distance weakens the intermolecular interactions between them, typically dipolar interactions and π - π stacking.

Composite PBLG/toluene gels were obtained by incorporation of PS into the solution. It was found that PBLG/toluene gels have high PS loading capacity. Gel formation was observed upon incorporation of 82% by weight PS into the solutions. DSC results showed that addition of PS did not affect thermoreversibility of PBLG/toluene system and that PS did not affect the structure nucleation stage of the gelation. Viscosity and turbidity results showed that gelation occurs at shorter times in the presence of PS indicating that PS can affect the later stages of gelation. AFM and optical microscope images confirmed the formation of branching network of PBLG molecules in PS matrix.

More need to be done for future. The nature of the intermolecular interactions causing fibrils to form 3D network still awaits an answer. We did try to investigate intermolecular interactions between PBLG molecules using FTIR, but could not get any convincing data to understand the nature of the interactions. We attempted to detect the arrangement of PBLG molecules in fibrillar structure by AFM, however it was not possible to observe individual PBLG molecules in the fibers. On the other hand, to understand the effect of PS incorporation precisely, different molecular weights of PS should be used to study more systematically. In addition, the effect of PS on PBLG/toluene gelation in molecular level still needs to be understood.

BIBLIOGRAPHY

1. Hamley, I.W., *Introduction to soft matter: synthetic and biological self-assembling materials*, in *Synthetic and Biological Self Assembling Materials*, J.W.a.S. Ltd., Editor. 2007.
2. Weiss, M.G.a.R.G., *Molecular Organogels. Soft Matter Comprised of Low-Molecular-Mass gelators and Organic Liquids*. ACCOUNTS OF CHEMICAL RESEARCH, 2005. **39**(8): p. 489-497.
3. Vintiloiu, A., *Organogels and their use in drug delivery*. Journal of controlled release, 2008. **125**: p. 179-192.
4. Ilknur Karakutuk, O.O., *Macroporous rubber gels as a reusable solvents for the removal of oil from surface waters*. Reactive and Functional Polymers 2010. **70**: p. 585-595.
5. Savin, S.S.N.a.D.A., *Poly(Z-lysine) - Based Organogels: Effect of Interfacial Frustration on Gel Strength* Macromolecules, 2009. **42**: p. 7114-7121.
6. Suzan Abdurrahmanoglu, V.C., Oguz Okay, *Design of high-toughness polyacrylamide hydrogels by hydrophobic modification*. Polymer, 2009. **50**: p. 5449-5455.
7. Ahn, S., *Stimuli-responsive polymer gels*. Soft Matter, 2008. **4**: p. 1151-1157.
8. Bhattacharya, S., *Modulation of Viscoelastic Properties of Physical Gels by Nanoparticle Doping: Influence of the Nanoparticle Capping Agent*. Angewandte Chemie International Edition, 2006. **44**: p. 7964-7968.
9. Ferry, J.D., *Viscoelastic properties of polymers*. Third ed. 1980, New York: John Wiley & Sons.
10. Moniruzzaman, M., *Improved mechanical strength and electrical conductivity of organogels containing carbon nanotubes*. CARBON, 2009. **47**: p. 645-650.
11. Gong, J.P., *Double Network Hydrogels with Extremely High Mechanical Strength*. Advanced Materials, 2003. **15**(14): p. 1155-1158.

12. Russo, P.S., *A Perspective on Reversible Gels and Related Systems*, in *REVERSABLE POLYMERIC GELS AND RELATED SYSTEMS*. 1987: Washington D.C. p. 1-21.
13. Llyod, J., *Colloid Chemistry*. 1926, New York: The Chemical Catalo Co.
14. Wu, X.S., *Synthesis and Characterization of Thermally Reversible Macroporus Poly(N-ISOPROPILACRYLAMIDE) Hydrogels*. *Journal of Polymer Science: Part A*, 1992. **30**: p. 2121-2129.
15. Qiu, Y., *Environment sensitive hydrogels for drug delivery*. *Advanced Drug Delivery Reviews*, 2001. **53**: p. 321-339.
16. Hoffman, A.S., *Hydrogels for biomedical applications*. *Advanced Drug Delivery Reviews*, 2002. **43**: p. 3-12.
17. Wang, Z., *Supramolecular Hydrogels Hybridized with Single-walled Carbon Nanotubes*. *Macromolecules*, 2007. **40**: p. 3402-3407.
18. Avishay Pelah, R.S., Thomas M.Jovin, *Reversible Cell Deformation by a Polymeric Actuator*. *Journal of the American Chemical Society*, 2007. **129**: p. 468-469.
19. Terech, P., *Low Molecular Mass Gelators of Organic Liquids and the Properties of their Gels*. *Chemical Reviews*, 1997. **97**(8): p. 3133-3159.
20. Liu, X.Y., *Formation Kinetics of Fractal Nanofiber Networks in Organogels*. *Applied Physics Letters* 2001. **79**: p. 3518-3520.
21. Cayley, A., *A Theorem on Trees*. *Quart. J. Math*, 1889. **23**: p. 376-378.
22. Gronwald, O., *Gelators for organic liquids based on self-assembly: A new faced of supramolecular and combinatorial chemistry*. *Current Opinion in Colloid & Interface Science*, 2002. **7**: p. 148-156.
23. Sangeetha, N.M., *Supramolecular gels: Functions and uses*. *Chemical Society Reviews*, 2005. **34**: p. 821-836.
24. Hill, A., *Differential scanning calorimetry and modulus measurements of poly(γ -benzyl-L-glutamate) gels*. *POLYMER*, 1988. **29**: p. 1426-1432.

25. Flory, P.J., *Face Equilibria in Solutions of Rod-like Particles*. Proceedings of the Royal Society A, 1956: p. 73-89.
26. Grace, D., *Topical diclofenac versus placebo: A double blind, randomized clinical trial inpatients with osteoarthritis of the knee*. J. Rheumatol, 1999. **26**: p. 2659-2663.
27. Schmidtke, S., *Thermoreversible Gelation of Isotropic and Liquid Crystalline Solutions of a "Sticky" Rodlike Polymer*. Macromolecules, 2000. **33**: p. 4427-4432.
28. Elliot, A., J. Disc. Faraday Soc., 1950. **9**: p. 246.
29. Poliks, M.D., Molcryst. Liq. Cryst., 1987. **153**: p. 321-346.
30. Duke, R.W., *Poly(γ -benzyl-L-glutamate) Helix-Coil Transition. Pretransition Phenomena in the Liquid Crystal Phase*. Journal of the American Chemical Society, 1976. **98**: p. 3094-3101.
31. Kohji Tohyama, W.G.M., *Network structure in gels of rod-like polypeptides*. Nature, 1981. **289**: p. 813-814.
32. Helfrich, J., *Molecular Dynamics Simulation Study of Poly(γ -benzyl-L-glutamate) in DMF*. Macromolecules, 1994. **27**: p. 472-482.
33. Floudas, G., *Hierarchical Self-Assembly of Poly(γ -benzyl-L-glutamate)-Poly(ethylene glycol)-Poly(γ -benzyl-L-glutamate) Rod-Coil-Rod Triblock Copolymers*. Macromolecules, 2003. **36**: p. 3673-3683.
34. Papadopoulos, P., *Self-Assembly and Dynamics of Poly(γ -benzyl-L-glutamate) Peptides*. Biomacromolecules, 2004. **5**: p. 81-91.
35. Gitsas, A., *Control of Peptide Secondary Structure and Dynamics in Poly(γ -benzyl-L-glutamate)-B-polyalanine Peptides*. Macromolecules, 2008. **41**: p. 8072-8080.
36. Tipton, D.L., *Thermoreversible Gelation of a Rod-like Polymer*. Macromolecules, 1996. **29**: p. 7402-7411.

37. Izumi, Y., *Two-Stage Melting in Dilute Gels of Poly(γ -benzyl-L-glutamate)*. *Macromolecules*, 1998. **31**(2): p. 430-435.
38. Cohen, Y., *Phase Transformation in Concentrated Solutions of Poly(γ -benzyl-L-glutamate)*. *Macromolecules*, 1995. **28**: p. 7638-7644.
39. Schmidt, M., *Combined Integrated and Dynamic Light Scattering by Poly(γ -benzyl-L-glutamate) in a Helicogenic Solvent*. *Macromolecules*, 1984. **17**: p. 553-560.
40. Russo, P.S., *Gelation of Poly(γ -benzyl-L-glutamate)*, in *Reversible Polymeric Gels and Related Systems*. 1987, American Chemical Society. p. 152-169.
41. Corenaga, T., *Spinodal Decomposition and Gel Structure of Quenched Poly(γ -benzyl-L-glutamate) Toluene Solutions*. *Journal of Macromolecular Science, Part B Physics*, 1997. **36**(4): p. 487-501.
42. Tadmor, R., *Reversible Gelation in Isotropic Solutions of the Helical Polypeptide Poly(γ -benzyl-L-glutamate): Kinetics and Formation Mechanism of the Fibrillar Network*. *Langmuir*, 2002. **18**: p. 7146-7150.
43. Horton, J.C., *Phase Separation in the Poly(γ -benzyl-L-glutamate)/benzyl alcohol system and its role in gelation*. *POLYMER*, 1991. **32**(13): p. 2418-2427.
44. Sasaki, S., *Molecular Aggregation and Gelation in Poly(γ -benzyl-L-glutamate) Solutions*. *Polymer Journal*, 1982. **14**(3): p. 205-213.
45. Russo, P.S., *On the Nature of Poly(γ -benzyl-L-glutamate)-Dimethylformamide "Complex Phase"*. *Macromolecules*, 1983. **17**(7): p. 1324-1331.
46. Shukla, P., *Thermodynamics and kinetics of gelation in the Poly(γ -benzyl-L-glutamate)-benzyl alcohol system*. *POLYMER*, 1992. **33**(2): p. 365-372.
47. Botiz, I., *The influence of protic non-solvents present in the environment on structure formation of poly(γ -benzyl-L-glutamate) in organic solvents*. *Soft Matter*, 2008. **4**: p. 993-1002.

48. Kim, K.T., *Gelation of Helical Polypeptide-Random Coil Diblock Copolymers by a Nanoribbon Mechanism*. *Angewandte Chemie International Edition*, 2005. **44**: p. 7964-7968.
49. Iijima, S., *Helical microtubules of graphitic carbon*. *Nature*, 1991. **354**: p. 56-58.
50. *Zetasizer Nano Series User Manual*. 2004.
51. *Instruction Manual AMVn Automated Viscometer*. 2005, Graz, Austria: Anton Paar GmbH
52. Höhne, G., *Differential Scanning Calorimetri*. 2003, New York: Springer.
53. Oikawa, H., *Dynamic Light Scattering Study on Sol-Gel Transition of Poly(γ -benzyl-L-glutamate)-toluene Solutions*. *Journal of Macromolecular Science, Part B Physics*, 1997. **36**(1): p. 87-101.
54. Breen, J.J., *Scanning Tunneling Microscopy Studies of the Synthetic Polypeptide Poly(γ -benzyl-L-glutamate)*. *Journal of Physical Chemistry*, 1992. **96**: p. 6825-6829.
55. Muthukumar, A.K.M.a.M., *Dynamic Mechanical Properties of Poly (γ -benzyl-L-glutamate) Macromolecules*, 1987. **20**: p. 564-569.
56. Janaky Narayanan, J.-Y.X.a.X., *Determination of agarose gel agarose pore size: Absorbance measurements vis a vis other techniques*. *Journal of Physics : Conference Series* 2006. **28**: p. 83-86.
57. Joshi, S.C., *Modelling Heat and Degree of Gelation for Methyl Cellulose Hydrogels with NaCl Additives*. *Journal of Applied Polymer Science*, 2006. **101**: p. 1620-1629.
58. Terech, P., *Thermoreversible Gelation of Organic Liquids by Arylcyclohexanol Derivatives: a Structural Study*. *Langmuir*, 1998. **14**: p. 3991-3998.
59. L., M., *Crystallization of polymers*. , ed. McGraw-Hill. 1963, New York.
60. al., L.G.e., *Growth and form of spherulites*. *Physical Review E*, 2005. **72**.

61. Donald, D.A.P.a.A.M., *Infrared Study of Molecular Aggregation in the poly (alpha-benzyl-L-glutamate) systems*. *Macromolecules*, 1993. **26**(8): p. 1947-1955.
62. Kenji Suzuki, K.T., Yukip Furukuwa, *Fiel-effect transistor configuration for the measuremeny of infrared Stark spectra*. *SCIENCE AND TECHNOLOGY OF ADVANCED MATERIALS*, 2006. **7**: p. 456-460.
63. Alexander, M.N., *A Large Single Crystal of Poly(γ -benzyl L-glutamate)*. 1977.
64. Jeong, B., *Thermoreversible Gelation of PEG-PLGA-PEG Triblock Copolymer Aqueous Solutions*. *Macromolecules*, 1999. **32**: p. 7064-7069.
65. Samanta, S.K., *Carbon nanotube reinforced supramolecular gels with electrically conducting, viscoelastic and near-infrared sensitive properties*. *Journal of Materials Chemistry*, 2010. **20**: p. 6881-6890.
66. Jans, H., *Dynamic Light Scattering as a Powerful Tool for Gold Nanoparticle Bioconjugation and Biomolecular Binding Studies*. *Analytical Chemistry*, 2009. **81**(22): p. 9425-9432.

VITA

Merve Kocakuşakoğulları was born in 1985, in Turkey. She graduated from Sırrı Yırcalı Anadolu Lisesi in 2003. Same year, she started her study in Chemistry department at Bilkent University, Ankara. In 2008, she received her B.S. degree and started her MS degree in Material Science and Engineering department at Koç University.